

This is the peer reviewed version of the following article:

Geyer, F., D'Acunzi, M., Yang, C.-Y., Mueller, M., Baumli, P., Kaltbeitzel, A., et al. (2019). How to Coat the Inside of Narrow and Long Tubes with a Super-Liquid-Repellent Layer-A Promising Candidate for Antibacterial Catheters. *Advanced Materials*, 31(2): 1801324. doi:10.1002/adma.201801324.

, which has been published in final form at: [10.1002/adma.201801324](https://doi.org/10.1002/adma.201801324)

## How to Coat the Inside of Narrow and Long Tubes with a Super Liquid-Repellent Layer - A Promising Candidate for Antibacterial Catheters

Florian Geyer, Maria D'Acunzi, Ching-Yu Yang, Michael Müller, Philipp Kaltbeitzel, Noemí Encinas, Doris Vollmer\*, and Hans-Jürgen Butt

Advanced Materials, 31\_(2): 1801324. doi:10.1002/adma.201801324.

## How to Coat the Inside of Narrow and Long Tubes with a Super Liquid-Repellent Layer – A Promising Candidate for Antibacterial Catheters

Florian Geyer, Maria D’Acunzi, Ching-Yu Yang, Michael Müller, Philipp Baumli, Anke Kaltbeitzel, Noemí Encinas, Doris Vollmer\*, and Hans-Jürgen Butt

Florian Geyer, Dr. Maria D’Acunzi, Dr. Ching-Yu Yang, Michael Müller, Philipp Baumli, Dr. Anke Kaltbeitzel, Dr. Noemí Encinas, Prof. Doris Vollmer, Prof. Hans-Jürgen Butt  
Max Planck Institute for Polymer Research, Ackermannweg 10, 55128 Mainz, Germany  
E-mail: vollmerd@mpip-mainz.mpg.de and butt@mpip-mainz.mpg.de

Keywords: wetting, superhydrophobic, superoleophobic, medical, anti-biofouling

Fouling of thin tubes is a major problem, leading to various infections and associated morbidities while cleaning is difficult or even impossible. Here we introduce a generic method to activate and coat the inside of meter-long and at the same time thin (down to 1 mm) tubes with a super liquid-repellent layer of nanofilaments, exhibiting even antibacterial properties. Activation is facilitated by pumping an oxidative Fenton solution through the tubes. Subsequent pumping of a silane solution renders the surface super liquid-repellent. Wide applicability of the method is demonstrated by coating stiff and flexible tubes made of polymers, inorganic/organic hybrids, metals and ceramics. Coated medical catheters show excellent antibacterial properties. Notably, the nanofilaments retain their antibacterial properties even in the superhydrophilic state. These findings open new avenues towards the design of biocide-free, antibacterial tubings and catheters.

Pipes, tubes, capillaries and hoses (in the following summarized as tubes) of different shapes and materials are essential for our daily life and numerous industrial processes. For example, thin tubes are used for food processing, water filtration<sup>[1]</sup>, gas separation,<sup>[2]</sup> microfluidics<sup>[3]</sup> or as insulating material. In medicine, the use of polymeric tubes is inevitable, for example for

infusions or catheters.<sup>[4]</sup> An ideal coating permits to tune the flow,<sup>[3, 5]</sup> the wetting properties,<sup>[6]</sup> and to suppress biofilm formation.<sup>[7]</sup> As cleaning of thin tubes is challenging or even impossible, the development of improved coatings is a pressing issue. Some super liquid-repellent layers can effectively hinder or delay biofilm formation, which is the irreversible attachment and proliferation of bacteria,<sup>[8]</sup> thereby diminishing the risk of infection-related problems (failure and replacement of implants or devices, and even sepsis). Thus, a promising strategy might be to coat the inside of tubes with a super liquid-repellent layer. Applying such a coating may suppress biofilm formation and thus save the life of thousands of patients in hospitals and retirement homes through reduction of pathogenic infections. Although several methods exist to coat an open surface with a super liquid-repellent layer,<sup>[9, 10]</sup> no technique is described which allows coating the inside of meter-long and narrow medically relevant tubes (diameter down to 1 mm). Here, we introduce a generic method to overcome this challenge.

Characteristic for super liquid-repellent coatings are their outstanding self-cleaning properties.<sup>[5, 11]</sup> When placing drops of water or complex liquids like blood on such a surface, the drop takes an almost spherical shape and rolls off, when the surface is tilted by less than 10°.<sup>[10, 12]</sup> To render a surface super liquid-repellent, it needs to be coated with nano- or micrometer-sized protrusions with overhanging morphology and low surface energy.<sup>[13]</sup> Such topology generates an energy barrier for the liquid so that water drops rest on the protrusions entrapping air underneath. As a result of this so-called Cassie state,<sup>[14]</sup> the liquid is more in contact with air rather than with a solid leading to high apparent contact angles.<sup>[15]</sup> Current methods to generate superhydrophobic and super liquid-repellent coatings on non-tubular substrates, such as electrospinning,<sup>[10]</sup> lithography,<sup>[16]</sup> dip coating,<sup>[17]</sup> spin coating,<sup>[18]</sup> or spray coating<sup>[19]</sup> are unsuitable for tubes having an inner diameter of only a few millimeters. Chemical etching methods of metal pipes, for example copper,<sup>[20]</sup> can produce microroughness. Nonetheless, etching is limited to the respective metal and metal tubes are rigid and prone to corrosion. Other techniques require activation of the surface, a challenge for long and narrow

polymeric tubes. Piranha cleaning solutions (a mixture of sulfuric acid, water and hydrogen peroxide) are suitable for glass surfaces but are unsuited for narrow tubes due to pronounced gas production and cannot effectively activate polymeric surfaces. Plasma activation is only applicable to activate short tubes as the plasma cannot be inducted inside of high aspect ratio tubes. Being able to coat the inside of high aspect ratio tubes will extend the range of applications of super liquid-repellent surfaces.<sup>[20, 21]</sup>

Here, we develop a universal route to activate and subsequently coat the inside of meter-long and at the same time thin tubes (down to 1 mm) with a super liquid-repellent layer of nanofilaments. Activation of long tubes was enabled by making use of the Fenton reaction which can be pumped through the tubes. Wide applicability of the coating method was demonstrated for tubes consisting of various materials, including polymers, hybrid materials, metals and ceramics. Excellent anti-biofouling properties were demonstrated using nanofilament-coated polyurethane catheters used in hospital.

To coat the inside of the tubes with a super liquid-repellent layer of nanofilaments the surface needs to be hydrophilic, having polar functional groups; preferentially hydroxy groups. Thus hydrophobic, unfunctionalized polymer surfaces need to be activated. Short polymer tubes can be activated via oxygen plasma, because the ionizing plasma can sufficiently penetrate from the ends of the tube. Plasma activation leads to the formation of various functional groups like hydroxy, carboxy, carbonyl and peroxy through radicalic action. After activation, the standard procedure (**Figure 1**) to coat tubes with a layer of silicone nanofilaments is to immerse the hydrophilic tubes in a solution of trichloromethylsilane (TCMS), in toluene or *n*-hexane for example, in the presence of trace amounts of water (85–225 ppm). After a reaction time of at least one hour the surface is covered with a layer of nanofilaments having a thickness of a few micrometers. During the reaction, the TCMS hydrolyzes, inducing a polysiloxane (i.e. silicone) polymerization on the surface of the tube (Figure S1 summarizes the involved chemical

reactions). The coating is superhydrophobic as the methyl groups of the polysiloxane orient to the outside to lower the surface energy<sup>[22]</sup>. To render the coating super liquid-repellent towards surfactant solutions or blood, the nanofilament-coated tubes are activated and modified with a perfluoro silane (*1H,1H,2H,2H*-perfluorodecyltrichlorosilane; see Figure S1 for XPS spectra of as-synthesized, plasma-activated and fluorinated nanofilaments in a tube).

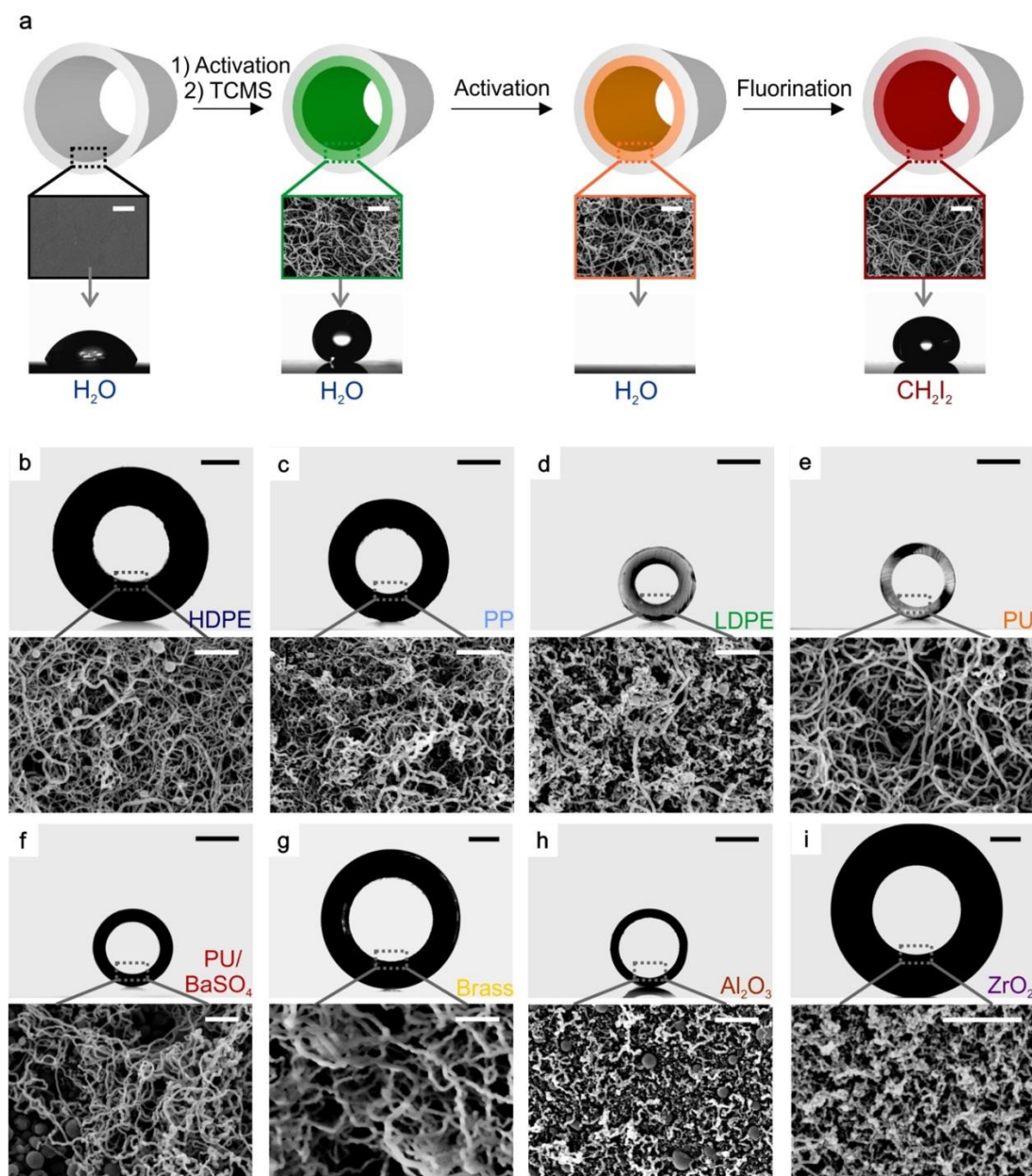


**Figure 1.** Illustration of the coating procedure, cross-sectional optical images and scanning electron microscopic (SEM) images of the inner surface of the nanofilament-coated tubes. a) After activation, the nanofilament coating can be applied by immersing in or flushing the tubes with a trichloromethylsilane solution for a certain reaction time. SEM images demonstrate the formation of nanofilaments. Subsequent activation and fluorination yield a super liquid-repellent coating. The different colors mark the change of the surface chemistry or topography of the interior surface. The photographs of the drops illustrate the changes of the wetting properties after each individual step on a flat surface. b) High-density polyethylene (HDPE) tube. c) Polypropylene (PP) tube. d) Low-density polyethylene (LDPE) tube. e) Polyurethane (PU) tube. f) Polyurethane/barium sulfate (PU/BaSO<sub>4</sub>) tube. g) Brass tube. h) Alumina (Al<sub>2</sub>O<sub>3</sub>) ceramic tube. i) Zirconia ceramic (ZrO<sub>2</sub>) tube. All SEM images show the formation of nanofilaments having diameters between 10–100 nm on the inner surface of the tubes. Scale bars: a) 500 nm; b–i) 200 nm for SEM images; 1 mm for optical images.

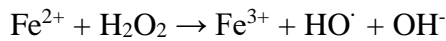
Notably, fluorinated nanofilaments can also be achieved in a one-step reaction<sup>[23]</sup> as verified by coating high-density polyethylene with filaments (Figure S2). Here, a mixture of tetraethoxysilane (TEOS) and 1*H*,1*H*,2*H*,2*H*-perfluorodecyltrichlorosilane (PFDTs) in toluene was used, containing trace amounts of water (100±5 ppm). TEOS and PFDTs hydrolyze due to the water traces in solution, inducing a polymerization on the surface of the tube, co-assembling into nanofilamentous structures.

Wide applicability of the method is demonstrated by coating tubes of varied materials having diameters between 1 mm and 3 mm. We applied the coating on commonly used and medically relevant polymer tubes, ranging from high-density polyethylene (HDPE), polypropylene (PP), low-density polyethylene (LDPE), and polyurethane (PU) to organic/inorganic hybrid polyurethane/BaSO<sub>4</sub> (Figure 1b–f). The PU and PU/BaSO<sub>4</sub> tubes are used in hospital as catheter

tubes, with BaSO<sub>4</sub> as X-ray contrast medium. In addition, the coating was applied to rigid brass, alumina (Al<sub>2</sub>O<sub>3</sub>), zirconia (ZrO<sub>2</sub>) and copper (Cu) tubes (Figure 1g–i; Figure S9 for Cu).

The HDPE, PP, LDPE and ceramic tubes were coated using TCMS (21 mmol L<sup>-1</sup>) dissolved in toluene with 135±10 ppm water content for 3 and 20 h, respectively. The brass and copper tubes were coated using a water content of 225±5 ppm for 3h. The polyurethane tubes (PU and PU/BaSO<sub>4</sub>) were coated in a water-saturated (85±5 ppm water content) TCMS (10 mmol L<sup>-1</sup>) solution in *n*-hexane for 20 h, showing that nanofilaments grow in both, toluene and *n*-hexane. Scanning electron microscopic (SEM) images demonstrate the formation of nanofilaments on all tubes. On the HDPE, PP, and LDPE tubes a coating consisting of mainly thinner nanofilaments (10–30 nm diameter) and some lone thicker nanofilaments (40–70 nm diameter) was obtained (Figure 1a–d). On the polyurethane tubes, the diameter of the nanofilaments varied between 20 and 70 nm in diameter. In addition, few silicone nanoparticles between 150 and 500 nm diameter were found inside the coating (Figure 1e–f). On brass, the coating consisted of nanofilaments with ≈50 nm diameter (Figure 1g). Ceramic tubes showed rather short and thin nanofilaments between 15 and 40 nm diameter (Figure 1h–i). More detailed SEM images of the bare and coated tubes are shown in Figure S3–S12.

The necessity of activation is demonstrated for LDPE tubes as model system (**Figure 2**). Without activation only a few randomly distributed nanofilaments formed on LDPE (Figure 2a). After plasma-activation, a short tube is coated with a homogenous layer of nanofilaments (Figure 2b). However, plasma activation is only applicable inside of short tubes because of limitations of the plasmogenic flux to penetrate into longer tubes. Thus, a more versatile method to activate the inner surface of tubes of arbitrary length is required. Here, we introduce the Fenton reaction<sup>[24]</sup> for activating the surfaces. The Fenton reaction is industrially widely used to oxidize contaminants or to treat waste water.<sup>[25]</sup> Fenton’s reagent is an aqueous solution of hydrogen peroxide and ferrous iron. The ferrous iron acts as catalyst to produce hydroxyl radicals and hydroxide ions as byproduct:



These hydroxyl radicals have the second highest oxidation potential (redox potential 2.80 V) of all common oxidation agents, only surpassed by fluorine (redox potential 3.03 V). Similar to the oxygen plasma the hydroxyl radicals oxidize the polymeric surface inside the tubes introducing functional groups containing oxygen, like hydroxy, peroxy, and carboxy (Figure 2c). X-Ray photoelectron spectroscopy (XPS) spectra of a bare and Fenton-activated LDPE tube revealed an increase of oxygen-containing functional groups (Figure 2d). This is manifested in the increase of the ratio between the oxygen (O1s) peak to the carbon (C1s) peak. The structure of the nanofilament coating depends on the activation time with Fenton's reagent and thus on the density of oxygen-containing functional groups on the polymer surface. Already after 30 min of exposure to a Fenton solution ( $22 \text{ mmol L}^{-1}$   $\text{FeSO}_4$ ,  $0.43 \text{ mol L}^{-1}$   $\text{H}_2\text{O}_2$ , pH = 2.8, cooled in ice bath) under a flow rate of  $8 \text{ mL min}^{-1}$ , a coating featuring mostly thick nanofilaments ( $> 100 \text{ nm}$ ) could be obtained on a LDPE tube (Figure 2e and Figure S13). After 60 min exposure, the coating was composed of highly homogenous filaments with an average diameter just below 100 nm. After 90 min, the average nanofilament diameter decreased below 100 nm. After 120 and 180 min exposure to Fenton's solution the nanofilaments were thicker than 100 nm. In addition, nanoparticles started to form.

To coat a 2 m long and 1 mm thick LDPE tube, the inner surface was activated by pumping Fenton's reagent ( $22 \text{ mmol L}^{-1}$   $\text{FeSO}_4$ ,  $0.43 \text{ mol L}^{-1}$   $\text{H}_2\text{O}_2$ , pH = 2.8, 90 min, cooled in ice bath) through the tube at a flow rate of  $8 \text{ mL min}^{-1}$  (see Supporting Information for further details). After Fenton-activation, a TCMS-solution ( $21 \text{ mmol L}^{-1}$  in toluene,  $150 \pm 5 \text{ ppm}$  water content) was slowly pumped ( $0.1 \text{ mL min}^{-1}$ ) through the tube to ensure a homogenous coating and to prevent the depletion of silane within the tube. Indeed, SEM images taken at both endings of the tube and in the middle of the tube document the formation of nanofilaments along the inside of the tube, i.e. a tube having an aspect ratio of 2000:1 (Figure 2e and Figure S14). Due to the

ability to pump the Fenton solution and the coating solution through the tube, the whole coating procedure can be applied to tubes of greatly varying materials and aspect ratios. The Fenton reaction can also be applied to activate coated tube, i.e. to obtain superhydrophilic tubes, permitting a fast filling of the tubes. Therefore, we pumped a Fenton's reagent through the tube coated with filaments.

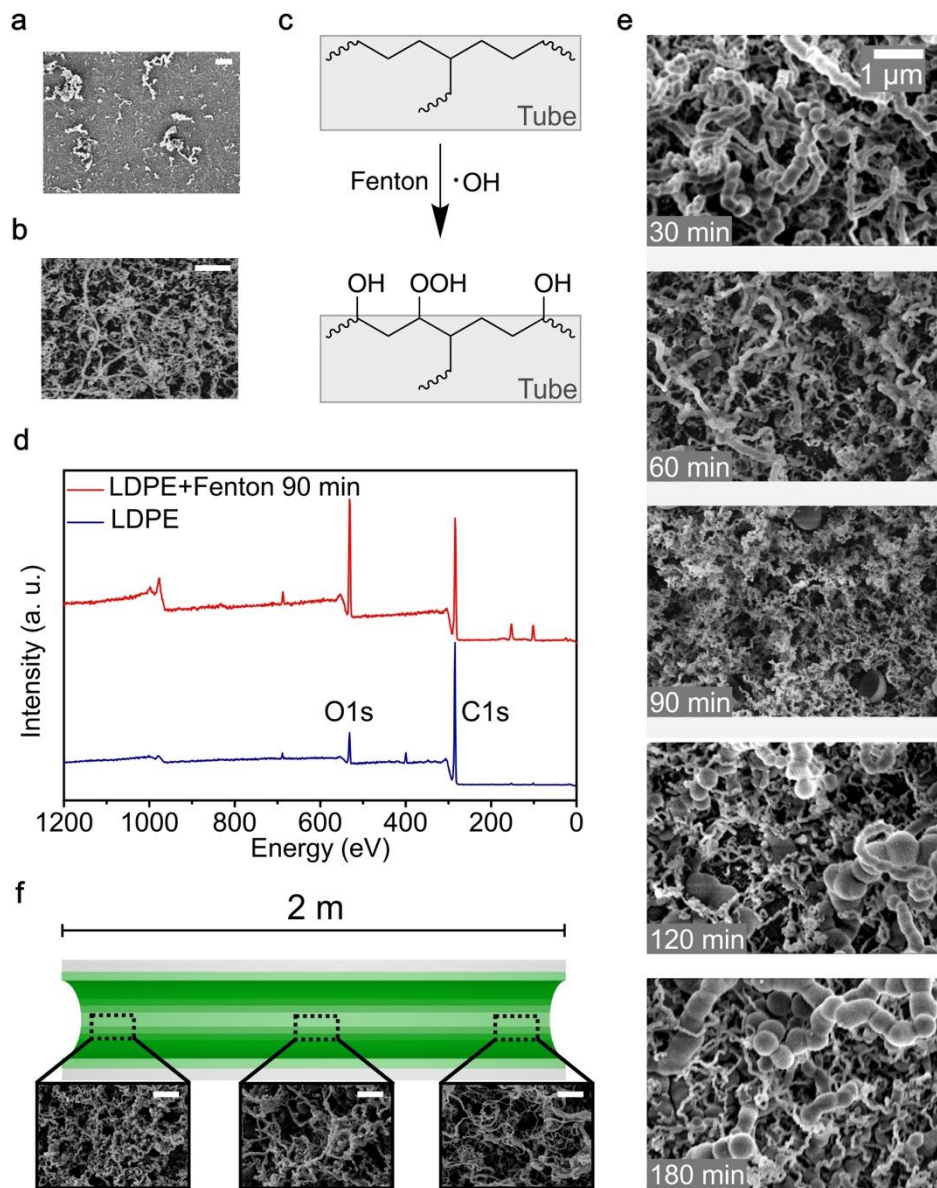


**Figure 2.** Activation and coating of a two meter-long tube. a) SEM image of low-density polyethylene (LDPE) tube coated without prior activation. b) SEM image of a short tube activated using oxygen plasma before the coating was applied. c) Scheme of the activation of

polymer surfaces using the Fenton reagent. d) X-Ray photoelectron spectroscopy (XPS) spectra of a bare and Fenton-activated LDPE tube. e) SEM images of coated Fenton-activated LDPE tubes after different Fenton reagent exposure times using a flow rate of  $8 \text{ mL s}^{-1}$ . f) SEM images of a coated LDPE tube with a total length of 2 m and an inner diameter of 1 mm at both endings and the middle of the tube. Formation of nanofilaments could be observed at all positions. Scale bars: a, b) 500 nm; f) 1  $\mu\text{m}$ .

The wetting properties of bare PU/BaSO<sub>4</sub> tubes and fluorinated nanofilaments on PU/BaSO<sub>4</sub> tubes were investigated using different liquids, relevant for biomedical applications (**Figure 3**). Due to the small inner diameter (1.3 mm) and the high curvature of the tubes, contact angles cannot be determined in a standard way, i.e. using the goniometer technique. However, super liquid-repellency is typically accompanied by only few pinning sites and low adhesion of drops to the surface. We quantified the wettability indirectly, by monitoring the adhesion of drops to the coating. Therefore, the tubes were horizontally cut in the middle prior to coating in order to avoid pinning sites at the cut surface. Drops of 2 or 3  $\mu\text{L}$  volume were placed onto the inside of the tubes. Next, the syringe was slowly moved up and down (see also Movie S1–S4). On bare PU/BaSO<sub>4</sub> tubes the high adhesion between the phosphate buffered saline (PBS, surface tension,  $\gamma = 0.072 \text{ N m}^{-1}$ ) and PU/BaSO<sub>4</sub> caused that the drop detached and stuck at the surface (Figure 3a). Contrary, on the tubes coated with fluorinated nanofilaments, drops of PBS, urine ( $\gamma = 0.060\text{--}0.066 \text{ N m}^{-1}$ ) and blood plasma ( $\gamma = 0.056 \text{ N m}^{-1}$ ) hardly showed any adhesion (Figure 3b–d). The drops could be easily removed by retracting the syringe. Drops of diiodomethane (CH<sub>2</sub>I<sub>2</sub>,  $\gamma = 0.051 \text{ N m}^{-1}$ ) detached from the syringe upon retraction and rolled out of the tube (Figure 3e). Detachment of the drops was caused by the high density of diiodomethane (3.3 g  $\text{mL}^{-1}$ ). The gravitational force exceeded adhesion of the drop to the needle. Super liquid-repellency (Figure Sx) towards common food liquids like water, cola, apple juice and non-polar liquid like iodobenzene ( $\gamma = 0.040 \text{ N m}^{-1}$ ) was verified using a coated

PU tube (Figure S15). That drops easily rolled out of the tube demonstrates the super liquid-repellency of the coating also to non-polar liquids. Optical imaging showed that all drops showed a lower adhesion than 3  $\mu\text{L}$  water drops on a superhydrophobic micropillar array (rectangular, 10  $\mu\text{m}$  height with  $5 \times 5 \mu\text{m}^2$  top areas; pillar-pillar distance 20  $\mu\text{m}$ ;  $9^\circ \pm 1^\circ$  roll-off angle for 6  $\mu\text{L}$  water drops). On micropillar arrays the drop either stuck to the surface or detachment of the drop from the surface caused visible vibrations of the drop (Movie S5). As a reference, we also measured the receding contact angles and roll-off angles on nanofilament-coated glass slides and on flat polyurethane/BaSO<sub>4</sub>. As a preparatory measure the tube material was flattened by heating. Phosphate buffered saline on flat PU/BaSO<sub>4</sub> showed a receding contact angle of  $43^\circ \pm 4^\circ$  and did not roll off. However, PBS on a nanofilament-coated glass slide showed a receding contact angle (RCA) of  $158^\circ \pm 4^\circ$  and a roll-off angle of  $2^\circ \pm 1^\circ$  for 6  $\mu\text{L}$  drops. After plasma- or Fenton-activation of the nanofilaments, the receding contact angle of PBS was  $\approx 0^\circ$ , due to super-spreading. On a glass slide coated with fluorinated nanofilaments, PBS and CH<sub>2</sub>I<sub>2</sub> as an example showed a receding contact angle of  $160^\circ \pm 4^\circ$  and  $149^\circ \pm 4^\circ$ , respectively and roll-off angles of  $1^\circ \pm 1^\circ$  and  $1^\circ \pm 1^\circ$  for 6  $\mu\text{L}$  drops, respectively. The extremely low adhesion of the drops to the coated inner surfaces of the tubes is in agreement with the high receding contact angles and low roll-off angles measured on nanofilament-coated glass slides.

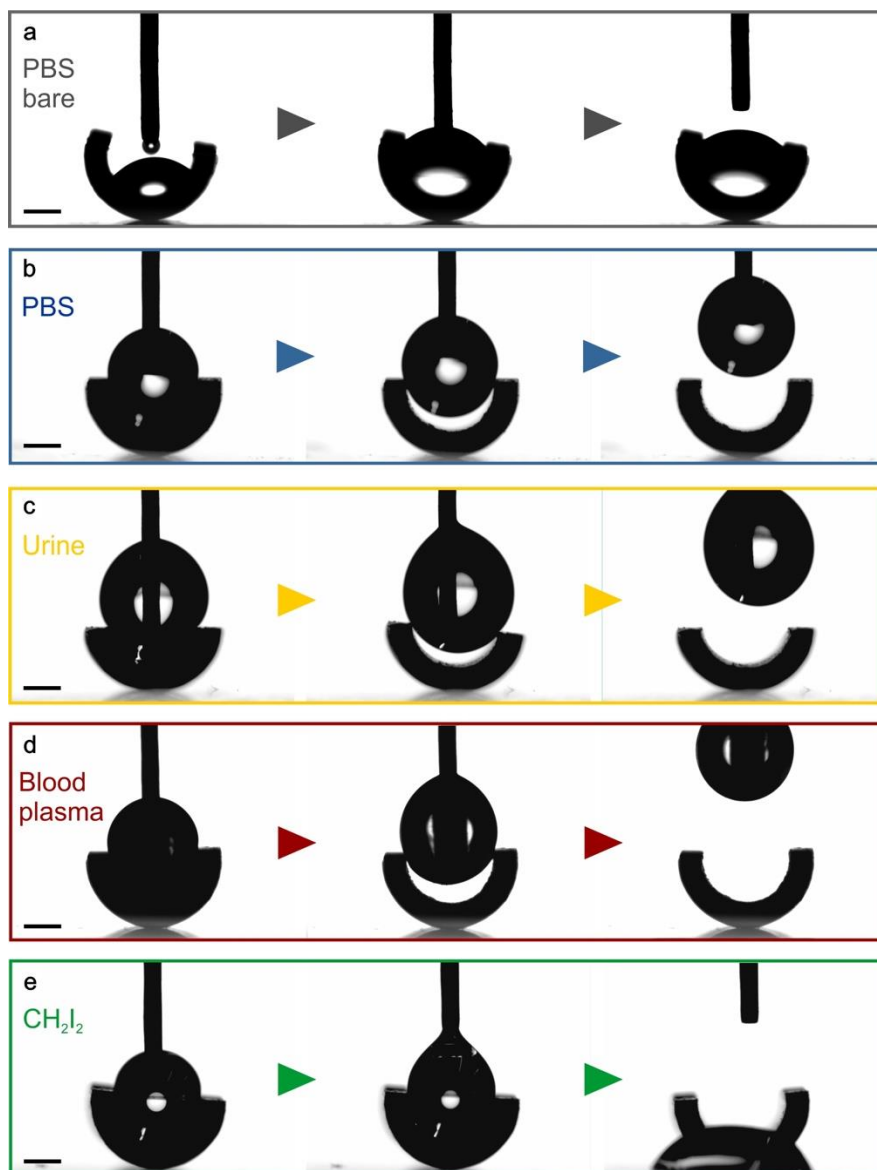


**Figure 3.** Wetting properties of a coated and fluorinated PU/BaSO<sub>4</sub> catheter tube in comparison to a bare PU/BaSO<sub>4</sub> tube. a) A 2 µL PBS (phosphate buffered saline) drop sticking on a bare tube. b,c) A 2 µL PBS and a 3 µL urine droplet on a coated tube; both showed very low adhesion and could be easily removed by retracting the syringe. d) Even a 2 µL blood plasma drop showed very low adhesion to a coated tube and was easily removed from it. e) A 2 µL diiodomethane drop on a coated tube; during retraction of the syringe the droplet detached from the syringe due to the high density of diiodomethane and rolled out of the tube. Scale bars: 0.5 mm.

Many super liquid-repellent coating suffer from a poor mechanical stability or easy delamination. To test the long-term stability of the coating against flow-induced shear, water was pumped through a nanofilament-coated LDPE tube (0.95 mm inner diameter) for up to 10 months (see supporting information for details). The flow was adjusted to the maximum accessible pumping speed of the peristaltic pump ( $11 \text{ mL min}^{-1}$ ) which corresponds to an average flow velocity of  $\approx 30 \text{ cm s}^{-1}$  and a shear rate at the tubes' inner surface of  $|\dot{\gamma}| \approx 2 \cdot 10^7 \text{ s}^{-1}$  and a shear force per unit area of  $\dot{\gamma}\eta = 2 \cdot 10^4 \text{ N m}^{-2}$  (here,  $\eta = 0.001 \text{ Pa}\cdot\text{s}$  is the viscosity of water; see Supporting Information and Figure S16 for further details). The morphology of the coating was checked after 5 d, 10 d, 30 days, 2, 3, and 10months (Figure S15). Surprisingly, even after 10 months, SEM images show that the morphology remained unaltered, which demonstrates the excellent adhesion of the nanofilaments to the substrate and the high stability of the coating. Tubes are typically exposed to bending. Therefore, we tested the flexibility of the coating towards bending. The coating did not alter, delaminate or break even after  $1000\times$  bending cycles (Figure S17). The methyl groups confer the flexibility to the coating (see SI for further details).

To evaluate the potential of the coated tubes regarding their anti-biofouling properties for medical devices, we incubated tubes in concentrated *E. coli* bacteria solutions ( $10^8 \text{ cells mL}^{-1}$ ) for 168 h at 37 °C. The samples included bare PU catheters as reference, as-prepared nanofilament-coated PU tubes (Me-NF), superhydrophilic nanofilament-coated PU tubes (OH-NF) and fluorinated nanofilament-coated PU tubes (F-NF) (Figure 4). After incubation, the inside of the bare PU tubes was homogeneously covered with *E. coli* (Figure 4a). On the nanofilament-coated tubes the coverage with *E. coli* was greatly reduced. Hardly any *E. coli* could be found (Figure 4b–d). The squares mark positions where a single bacterium was located. The *E. coli* bacteria had a few micrometers in length and adhered to the top faces of a few nanofilaments (Figure 4b, right). On the as-prepared and fluorinated nanofilaments, the number of adhered bacteria was reduced by more than 20 times. Notably, on the

superhydrophilic nanofilaments, the number of bacteria per  $\text{cm}^2$  was reduced by up to almost two orders of magnitude, 85 times (Figure 4e, see Supporting Information and Figure S17 for further details). Thus, the presented coating is capable of effectively reducing bacterial adhesion and biofilm formation in the superhydrophobic as well as in the fully wetted state, the so-termed Wenzel state. We attribute this excellent anti-biofouling property to the characteristic spacing of the irregular three-dimensional layer of nanofilaments which falls just below the size of *E. coli* (Figure 4b). Therefore, the stiff bacteria cannot enter the pores. Furthermore, the small diameter of the nanofilaments and their irregular three-dimensional arrangement reduces the anchoring area. This distinctive combination of length scales and morphology makes tubes coated with nanofilaments a highly promising candidate for medical applications, for example as catheter or stent.

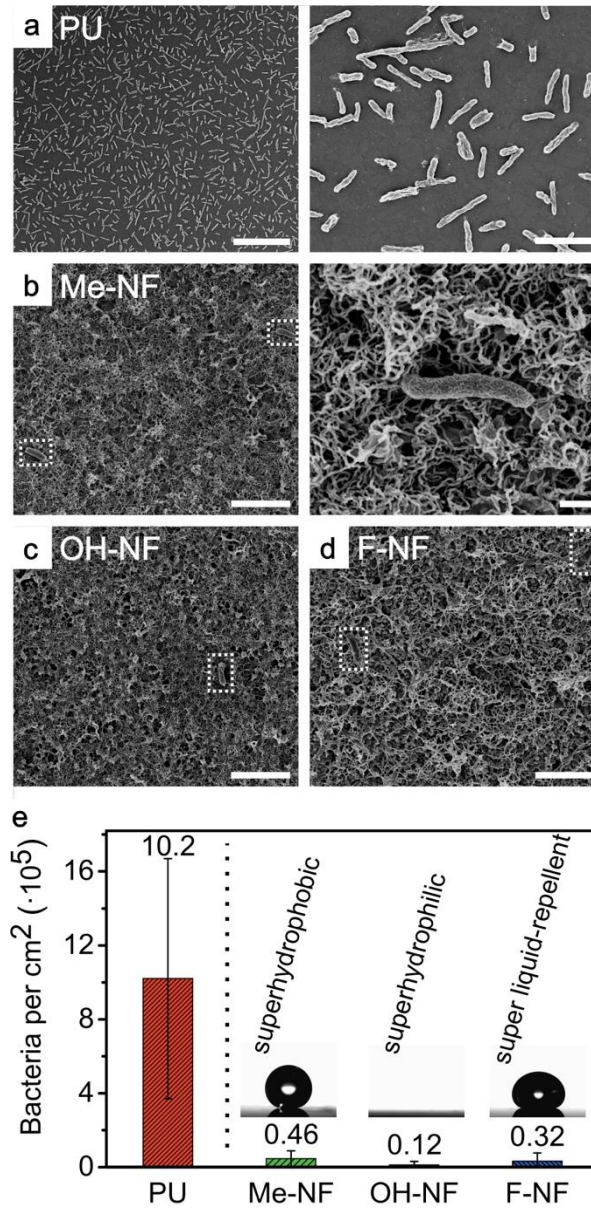


**Figure 4.** Antibacterial properties of a bare PU tube, a nanofilament-coated PU tube, a superhydrophilic nanofilament-coated PU tube and a fluorinated nanofilament-coated PU tube after an incubation time of 168 h in an *E. coli* solution. a) Bare PU tube showing high *E. coli* coverage. Scale bars: 20  $\mu\text{m}$  (left); 4  $\mu\text{m}$  (right). b) Nanofilament-coated PU tube showing highly reduced bacterial coverage (left). High magnification of a single *E. coli* bacterium attached on nanofilaments (right). Scale bars: 4  $\mu\text{m}$  (left); 500 nm (right). c) Superhydrophilic nanofilament-coated PU tube. Scale bar: 4  $\mu\text{m}$ . d) Fluorinated nanofilament-coated PU tube. Scale bar: 4  $\mu\text{m}$ . e) Average number of bacteria per area adhered to the surface for the different

tubes after 168 hours of incubation, documenting the superior antifouling properties of the coating. Error:  $\pm$ SD.

In conclusion, pumping Fenton's solution through thin polymeric tubes offers a versatile and simple method to activate their inner surfaces. The activated surfaces can subsequently be coated with a layer of nanofilaments. Due to the ability to pump both, the Fenton solution and the coating solution, the wetting properties of meter-long and at the same time thin tubes (here: 2 m with 1 mm diameter) or other bicontinuous surfaces can be tuned from superhydrophilic to super liquid-repellent. The Fenton activation may also be used to apply other liquid-repelling or antibacterial coatings, for example liquid-like PDMS<sup>[26]</sup> coatings. Pumping offers the possibility that the activation and the coating step can easily be parallelized. Hundreds of parallel arranged tubes can be treated simultaneously. Coated medical catheters prove to be promising candidates for reducing bacterial growth. Remarkably, even in the superhydrophilic state, the attachment of bacteria is highly reduced. Thus, the irregular 3D topography of nanofilaments greatly reduces the anchoring area for bacteria. Besides the excellent antibacterial properties, the coating can also withstand high flow velocities, bending and does not delaminate. The wide applicability of the nanofilament coating on tubes of various diameters and materials makes this method very useful for a broad range of applications. It opens new avenues to fabricate biocide-free coatings of medical devices as the reduced bacterial adhesion and proliferation reduces the infection risk of patients.

### Supporting Information

Supporting Information is available from the Wiley Online Library or from the author.

### Acknowledgements

This work was supported by the ERC Advanced Grant 340391 – SUPRO (H.-J.B.), the German Research Foundation (DFG) with the Collaborative Research Center 1194 (H.-J.B., F.G.), the European Union's Horizon 2020 research and innovation program LubISS No. 722497 (D.V.,

P.B.), the DAAD-MoST sandwich scholarship (C-Y.Y.) and the Marie Skłodowska-Curie fellowship 660523-NoBios-ESR (N.E.). Gabriele Schäfer and G. Glasser are acknowledged for technical support.

Received: ((will be filled in by the editorial staff))

Revised: ((will be filled in by the editorial staff))

Published online: ((will be filled in by the editorial staff))

## References

- [1] D. Menne, F. Pitsch, J. E. Wong, A. Pich, M. Wessling, *Anger. Chem. Int. Edit.* **2014**, 53, 5706.
- [2] A. Mansourizadeh, A. F. Ismail, *J. Hazard. Mater.* **2009**, 171, 38.
- [3] H. A. Stone, A. D. Stroock, A. Ajdari, *Annu. Rev. Fluid Mech.* **2004**, 36, 381.
- [4] E. H. Kass, L. J. Schneiderman, *N. Engl. J. Med.* **1957**, 256, 556.
- [5] B. Bhushan, Y. C. Jung, *Prog. Mat. Sci.* **2011**, 56, 1.
- [6] D. Bonn, J. Eggers, J. Indekeu, J. Meunier, E. Rolley, *Rev. Mod. Phys.* **2009**, 81, 739; P. G. de Gennes, *Rev. Mod. Phys.* **1985**, 57, 827; D. Quéré, *Ann. Rev. Mater. Res.* **2008**, 38, 71; X. Feng, L. Jiang, *Adv. Mater.* **2006**, 18, 3063.
- [7] J. W. Costerton, P. S. Stewart, E. P. Greenberg, *Science* **1999**, 284, 1318; L. D. Renner, D. B. Weibel, *MRS Bulletin* **2011**, 36, 347; D. C. Leslie, A. Waterhouse, J. B. Berthet, T. M. Valentin, A. L. Watters, A. Jain, P. Kim, B. D. Hatton, A. Nedder, K. Donovan, E. H. Super, C. Howell, C. P. Johnson, T. L. Vu, D. E. Bolgen, S. Rifai, A. R. Hansen, M. Aizenberg, M. Super, J. Aizenberg, D. E. Ingber, *Nat. Biotechnol.* **2014**, 32, 1134.
- [8] R. B. Pernites, C. M. Santos, M. Maldonado, R. R. Ponnappati, D. F. Rodrigues, R. C. Advincula, *Chemistry of Materials* **2012**, 24, 870; C.-Y. Loo, P. M. Young, W.-H. Lee, R. Cavaliere, C. B. Whitchurch, R. Rohanizadeh, *Acta Biomaterialia* **2012**, 8, 1881; X.-Q. Dou, D. Zhang, C. Feng, L. Jiang, *ACS Nano* **2015**, 9, 10664.
- [9] L. Feng, S. H. Li, Y. S. Li, H. J. Li, L. J. Zhang, J. Zhai, Y. L. Song, B. Q. Liu, L. Jiang, D. B. Zhu, *Adv. Mat.* **2002**, 14, 1857; X. Yao, Y. Song, L. Jiang, *Adv. Mater.* **2011**, 23, 719; T. Verho, C. Bower, P. Andrew, S. Franssila, O. Ikkala, R. H. A. Ras, *Adv. Mater.* **2011**, 23, 673; M. Paven, P. Papadopoulos, S. Schoettler, X. Deng, V. Mailaender, D. Vollmer, H.-J. Butt, *Nat. Commun.* **2013**, 4.
- [10] A. Tuteja, W. Choi, M. Ma, J. M. Mabry, S. A. Mazzella, G. C. Rutledge, G. H. McKinley, R. E. Cohen, *Science* **2007**, 318, 1618.
- [11] R. Fürstner, W. Barthlott, C. Neinhuis, P. Walzel, *Langmuir* **2005**, 21, 956; B. Bhushan, Y. C. Jung, K. Koch, *Langmuir* **2009**, 25, 3240.
- [12] X. Deng, L. Mammen, H.-J. Butt, D. Vollmer, *Science* **2012**, 335, 67; T. L. Liu, C.-J. C. Kim, *Science* **2014**, 346, 1096; K. Golovin, D. H. Lee, J. M. Mabry, A. Tuteja, *Angew. Chem. Int. Edit.* **2013**, 52, 13007.
- [13] C. W. Extrand, *Langmuir* **2004**, 20, 5013; D. Quéré, *Rep. Prog. Phys.* **2005**, 68, 2495; H.-J. Butt, C. Semprebon, P. Papadopoulos, D. Vollmer, M. Brinkmann, M. Ciccotti, *Soft Matter* **2013**, 9, 418; S. Herminghaus, *EPL* **2007**, 79.
- [14] A. B. D. Cassie, S. Baxter, *Trans. Faraday Soc.* **1944**, 40, 0546.
- [15] A. Lafuma, D. Quéré, *Nat. Mater.* **2003**, 2, 457; A. T. Paxson, K. K. Varanasi, *Nat. Commun.* **2013**, 4:1492.

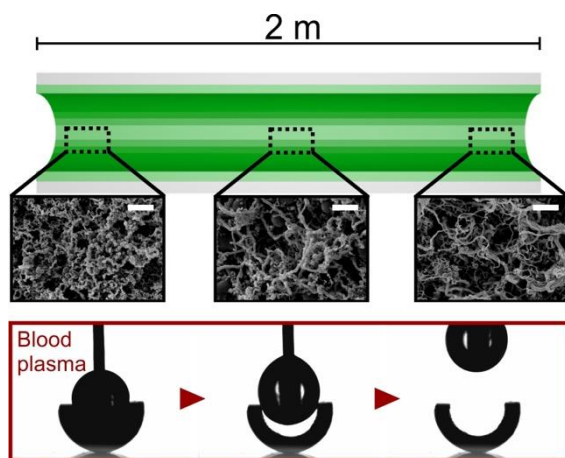
- [16] E. Martines, K. Seunarine, H. Morgan, N. Gadegaard, C. D. W. Wilkinson, M. O. Riehle, *Nano Lett.* **2005**, 5, 2097.
- [17] M. D'Acunzi, L. Mammen, M. Singh, X. Deng, M. Roth, G. K. Auernhammer, H.-J. Butt, D. Vollmer, *Faraday Discuss.* **2010**, 146, 35.
- [18] S. A. Kulinich, M. Farzaneh, *Applied Surface Science* **2009**, 255, 8153.
- [19] M. T. H. Teisala, M. Aromaa, J. M. Mäkelä, M. Stepien, J. J. Saarinen, M. Toivakka, J. Kuusipalo, *Surf. Coat. Technol.* **2010**, 205, 436; H. Teisala, M. Tuominen, M. Aromaa, M. Stepien, J. M. Mäkelä, J. J. Saarinen, M. Toivakka, J. Kuusipalo, *Langmuir* **2012**, 28, 3138.
- [20] N. J. Shirtcliffe, G. McHale, M. I. Newton, Y. Zhang, *ACS Appl. Mater. Inter.* **2009**, 1, 1316.
- [21] R. J. Daniello, N. E. Waterhouse, J. P. Rothstein, *Phys. Fluids* **2009**, 21, 085103.
- [22] G. R. J. Artus, S. Jung, J. Zimmermann, H.-P. Gautschi, K. Marquardt, S. Seeger, *Adv. Mater.* **2006**, 18, 2758; L. Gao, T. J. McCarthy, *J. Am. Chem. Soc.* **2006**, 128, 9052; J. Zhang, S. Seeger, *Angew. Chem. Int. Edit.* **2011**, 50, 6652; F. Geyer, C. Schönecker, H.-J. Butt, D. Vollmer, *Adv. Mater.* **2017**, 29.
- [23] J. Zhang, A. Wang, S. Seeger, *Polym. Chem.* **2014**, 5, 1132.
- [24] H. J. H. Fenton, *J. Chem. Soc., Trans.* **1894**, 65, 899.
- [25] J. J. Pignatello, E. Oliveros, A. MacKay, *Crit. Rev. Environ. Sci. Technol.* **2007**, 36, 1.
- [26] Wang, T. J. McCarthy, *Angew. Chem. Int. Ed.* **2017**, 55, 244.

An effective procedure to activate and coat the inside of thin and meter-long tubes with a super liquid-repellent layer consisting of nanofilaments is developed. Wide applicability to a broad range of materials is demonstrated. The biocide-free coating shows excellent stability against high flow velocities and successfully suppresses adhesion of bacteria as demonstrated by coated medical catheters.

### Coatings

Florian Geyer, Maria D'Acunzi, Ching-Yu Yang, Michael Müller, Philipp Baumli, Anke Kaltbeitzel, Noemí Encinas, Doris Vollmer\*, and Hans-Jürgen Butt

#### How to Coat the Inside of Narrow and Long Tubes with a Super Liquid Repellent Layer – A Promising Candidate for Antibacterial Catheters



Copyright WILEY-VCH Verlag GmbH & Co. KGaA, 69469 Weinheim, Germany, 2018.

## Supporting Information

### **How to Coat the Inside of Narrow and Long Tubes with a Super Liquid Repellent Layer – A Promising Candidate for Antibacterial Catheters**

Florian Geyer, Maria D’Acunzi, Ching-Yu Yang, Michael Müller, Philipp Baumli, Anke Kaltbeitzel, Noemí Encinas, Doris Vollmer\*, and Hans-Jürgen Butt

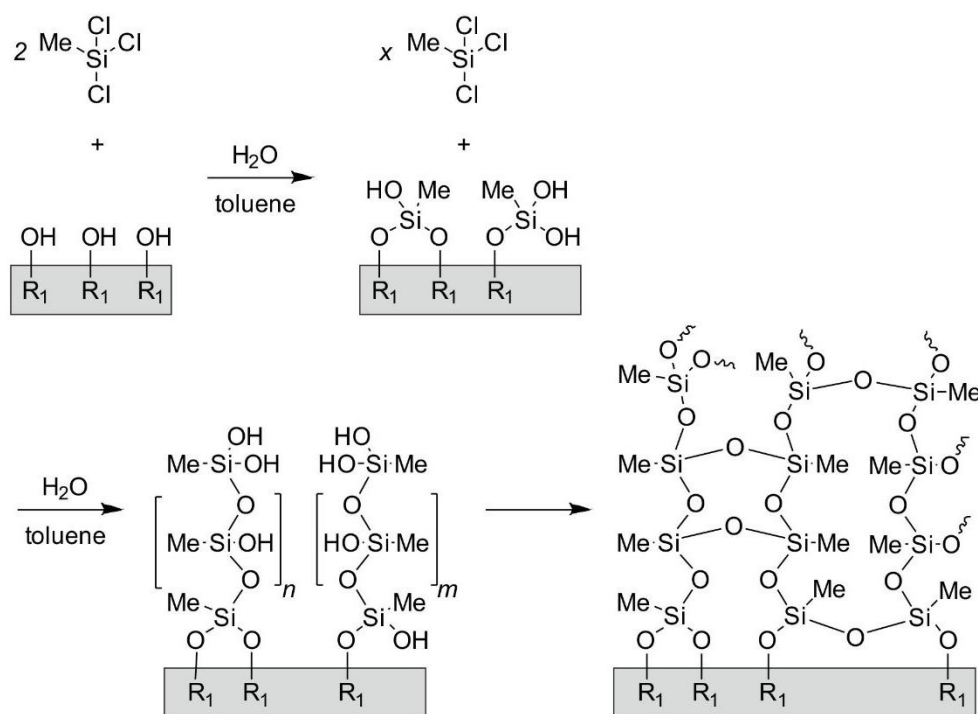


**Figure S1.** Possible reaction mechanism for the formation of nanofilaments.<sup>1,2</sup>

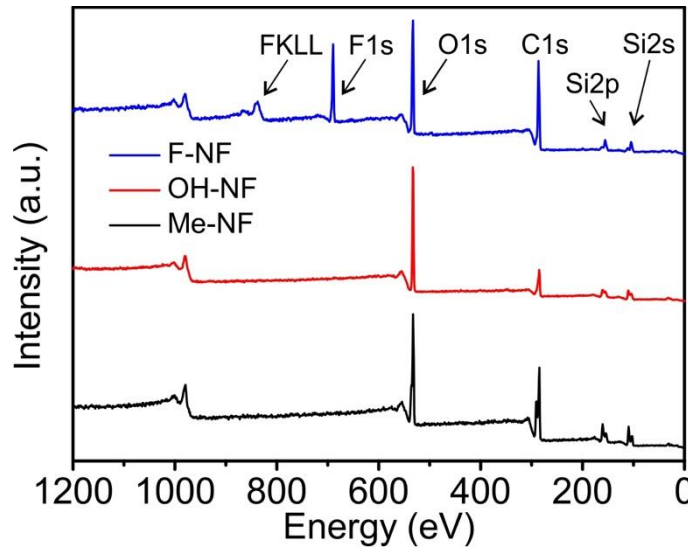


**Figure S2.** X-Ray photoelectron spectroscopy (XPS) spectra of as-synthesized nanofilaments (Me-NF), plasma-activated nanofilaments (OH-NF), and fluorinated nanofilaments (F-NF). Plasma-activated SNFs show a higher oxygen content compared to the as-synthesized nanofilaments. Fluorinated SNFs show the appearance of fluorine signals.

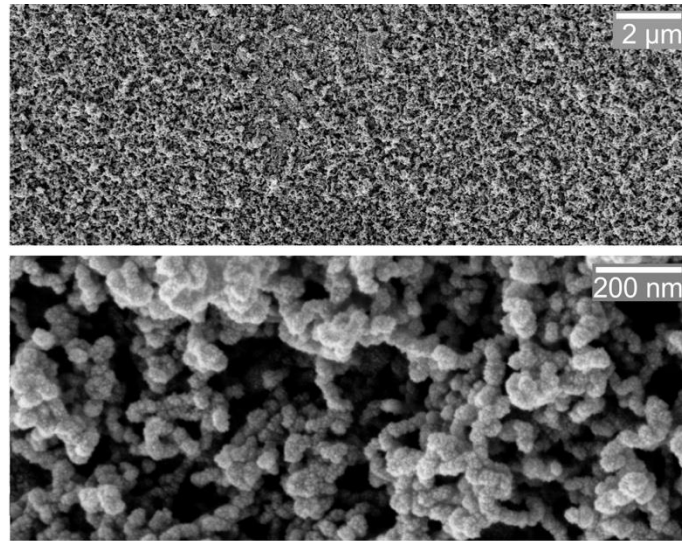


**Figure S3.** Scanning electron microscopic images (SEM) of the inside of a coated high-density polyethylene (HDPE) tube using a one-step reaction of TEOS and PFDTs. The filaments are composed of strings of nanoparticles.

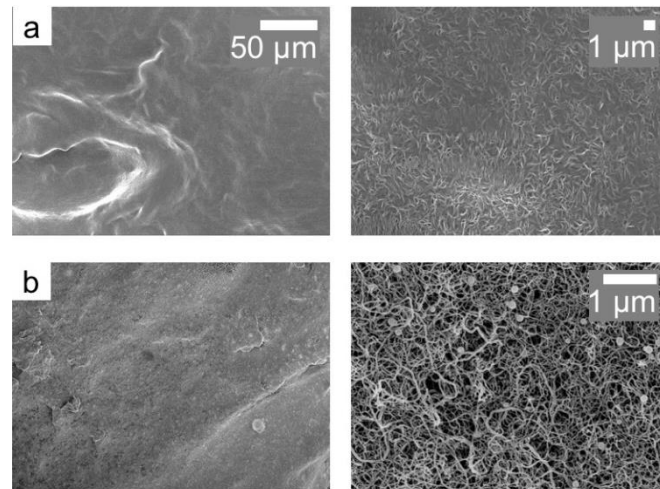


**Figure S4.** SEM images of the inside of bare and coated high-density polyethylene (HDPE) tubes. Bare (a) and coated (b) HDPE tube at different magnifications. For better comparison, the magnifications were chosen identical in (a) and (b) except for the right column.

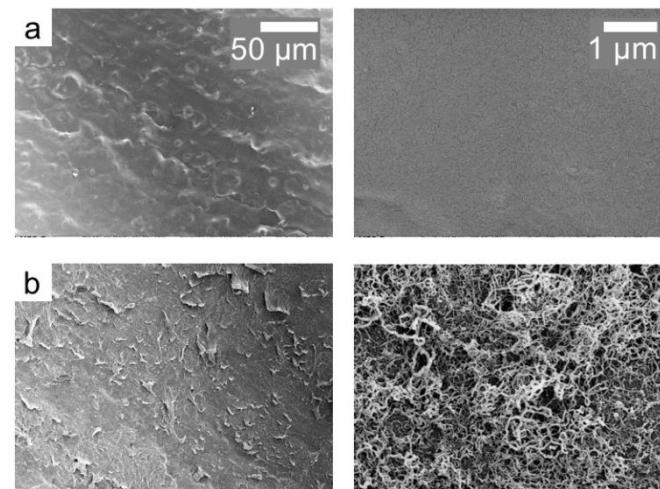


**Figure S5.** SEM images of the inside of bare and coated polypropylene (PP) tubes. Bare (a) and coated (b) PP tube at different magnifications. For better comparison, the magnifications were chosen identical in (a) and (b).

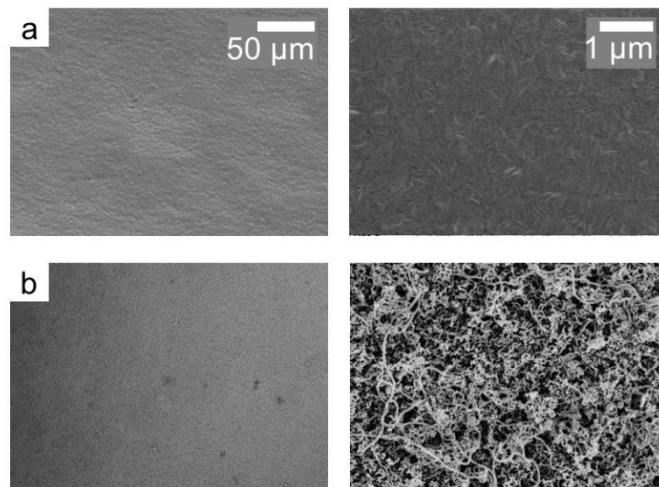


**Figure S6.** SEM images of the inside of bare and coated low-density polyethylene (LDPE) tubes. Bare (a) and coated (b) LDPE tube at different magnifications. For better comparison, the magnifications were chosen identical in (a) and (b).

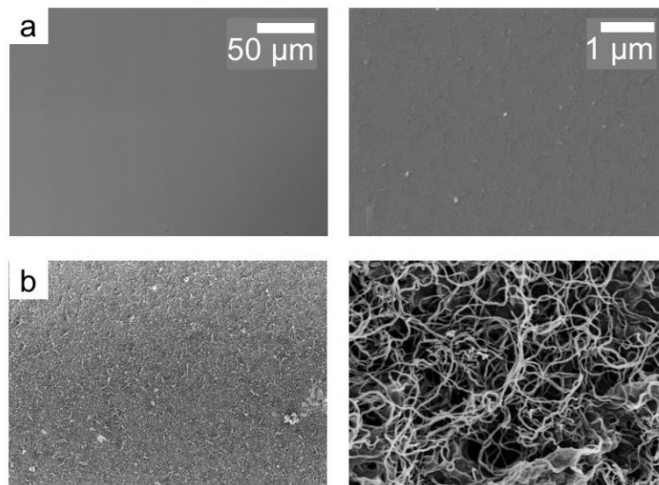


**Figure S7.** SEM images of the inside of bare and coated polyurethane (PU) tubes. Bare (a) and coated (b) PU tube at different magnifications. For better comparison, the magnifications were chosen identical in (a) and (b).

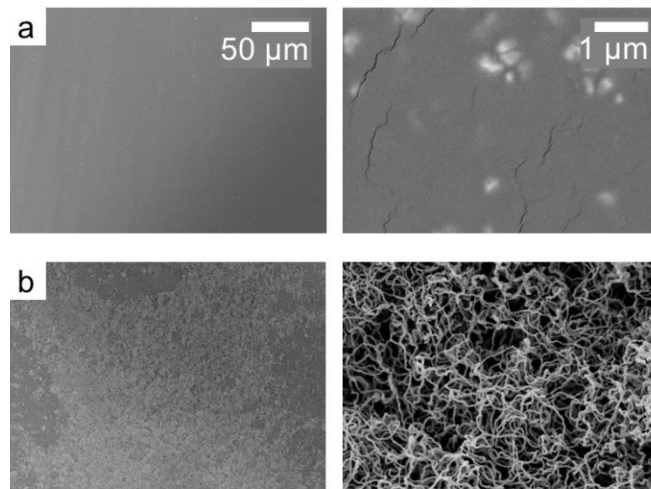


**Figure S8.** SEM images of the inside of bare and coated polyurethane/barium sulfate (PU/BaSO<sub>4</sub>) tubes. Bare (a) and coated (b) PU/BaSO<sub>4</sub> tube at different magnifications. For better comparison, the magnifications were chosen identical in (a) and (b).

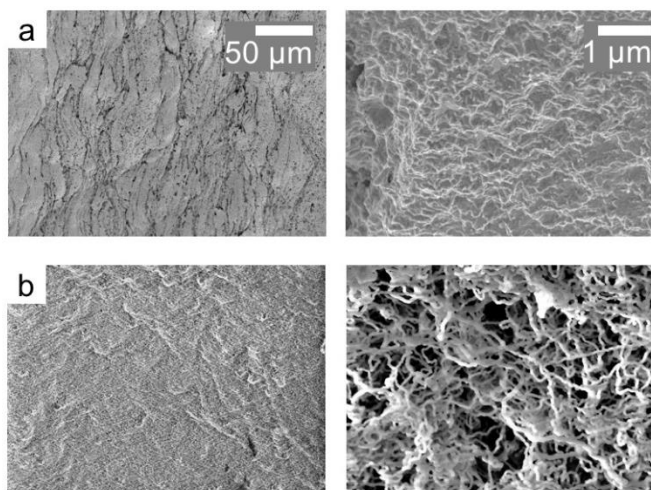


**Figure S9.** SEM images of the inside of bare and coated brass tubes recorded at an inclination of 45°. Bare (a) and coated (b) brass tube at different magnifications. For better comparison, the magnifications were chosen identical in (a) and (b).

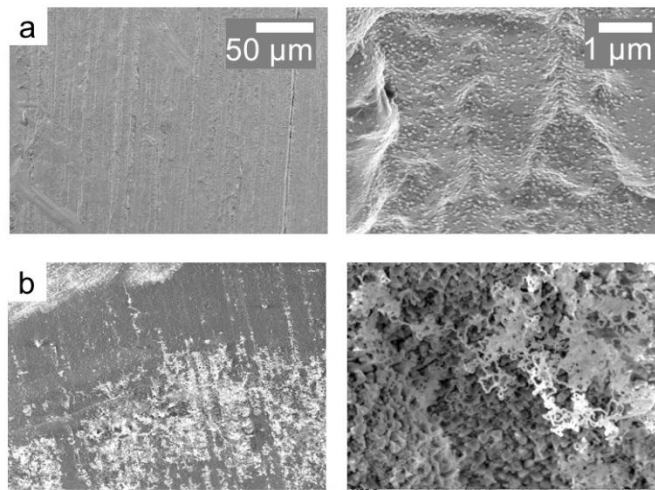


**Figure S10.** SEM images of the inside of bare and coated copper (Cu) tubes recorded at an inclination of 45°. Bare (a) and coated (b) Cu tube at different magnifications. For better comparison, the magnifications were chosen identical in (a) and (b).

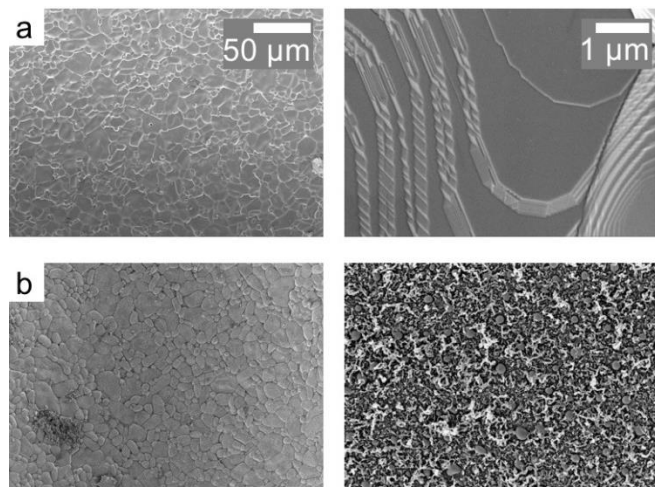


**Figure S11.** SEM images of the inside of bare and coated thin alumina ( $\text{Al}_2\text{O}_3$ ) tubes. Bare (a) and coated (b)  $\text{Al}_2\text{O}_3$  tube at different magnifications. For better comparison, the magnifications were chosen identical in (a) and (b).

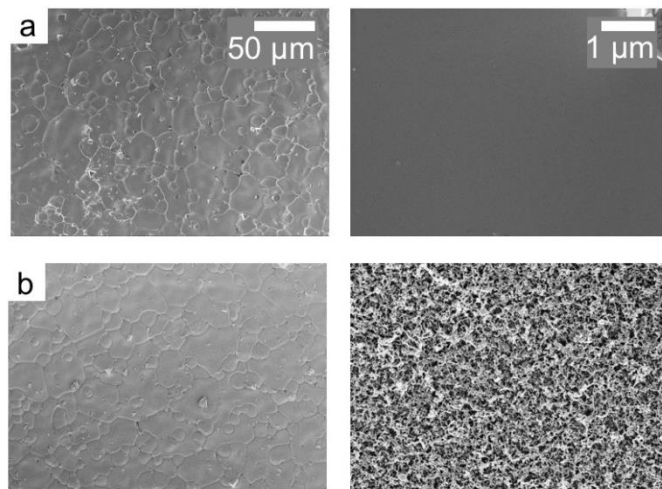


**Figure S12.** SEM images of the inside of bare and coated zirconia ( $\text{ZrO}_2$ ) tubes. Bare (a) and coated (b)  $\text{ZrO}_2$  tube at different magnifications. For better comparison, the magnifications were chosen identical in (a) and (b).

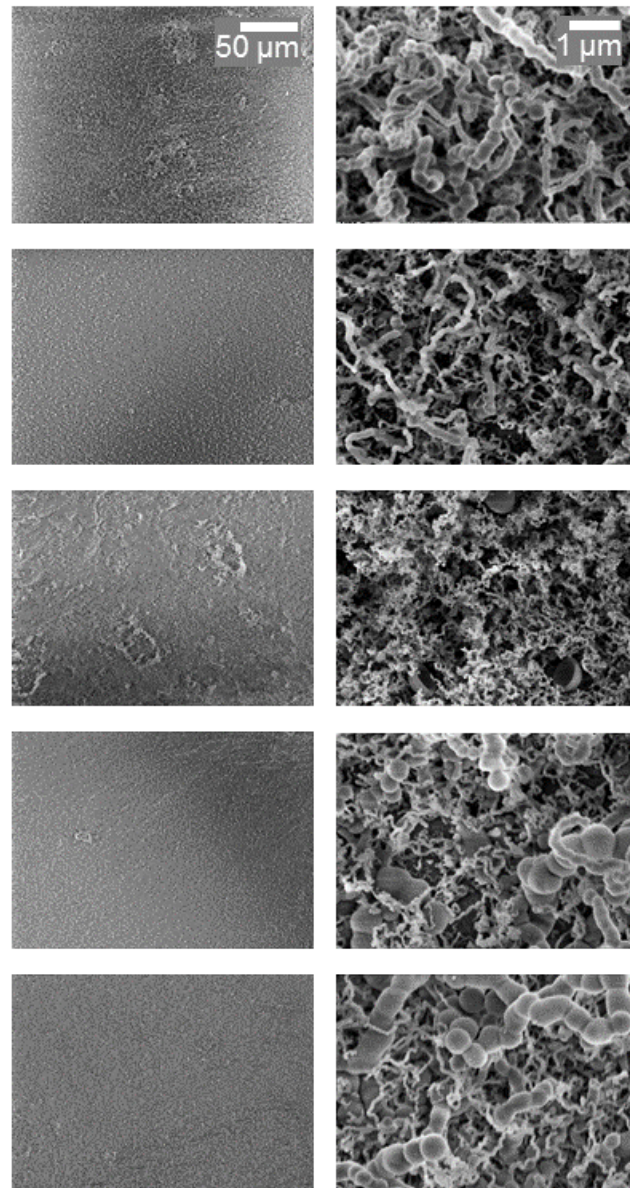


**Figure S13.** SEM images of the inside of coated Fenton-activated LDPE tubes after different Fenton exposure times under a flow of  $8 \text{ mL s}^{-1}$ . After the Fenton activation, the tubes were cut in short pieces ( $\approx 3 \text{ cm}$ ) and coated using the procedure described in the main text. The exposure times were 30 min (a), 60 min (b), 90 min (c), 120 min (d), and 180 min (e).

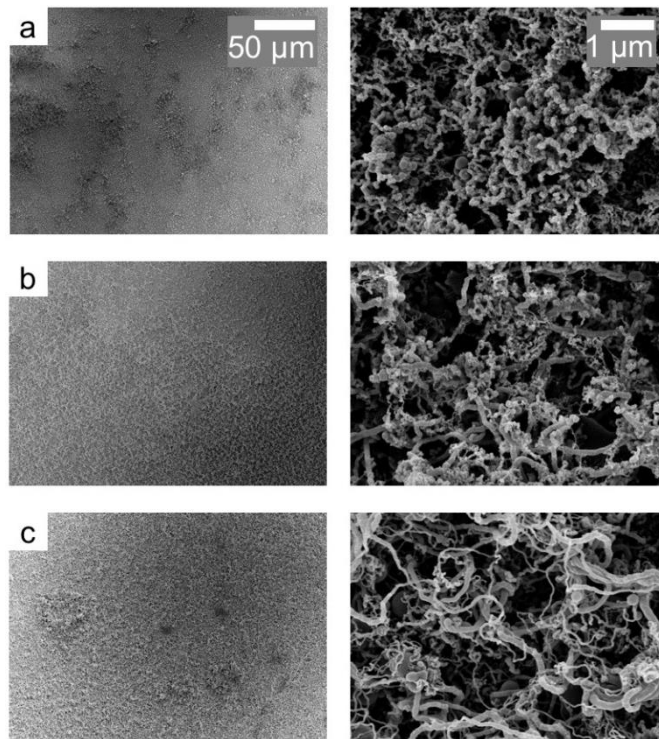


**Figure S14.** SEM images of the inside of the coated 2 m long LDPE tube. a,c) Images taken at both endings of the tube. b) Image taken at the middle of the tube. Formation of nanofilaments can be observed at all positions.

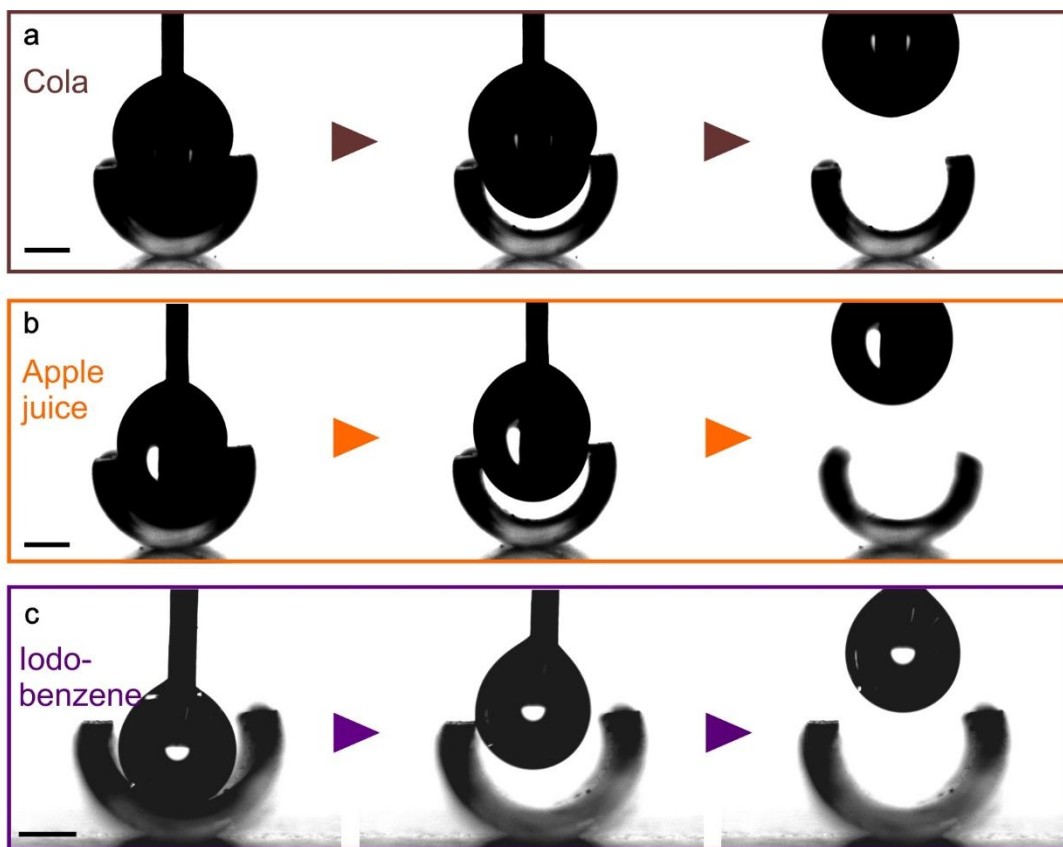


**Figure S15.** Wetting properties of a coated and fluorinated PU catheter. a,b) A  $\approx 2.5 \mu\text{L}$  Cola and a  $\approx 2 \mu\text{L}$  apple juice (with gas) droplet on a coated tube; both showed very low adhesion and could be easily removed by retracting the syringe. c) A  $1 \mu\text{L}$  iodobenzene shows high contact angles and low adhesion to the coated tube. Scale bars: 0.5 mm.

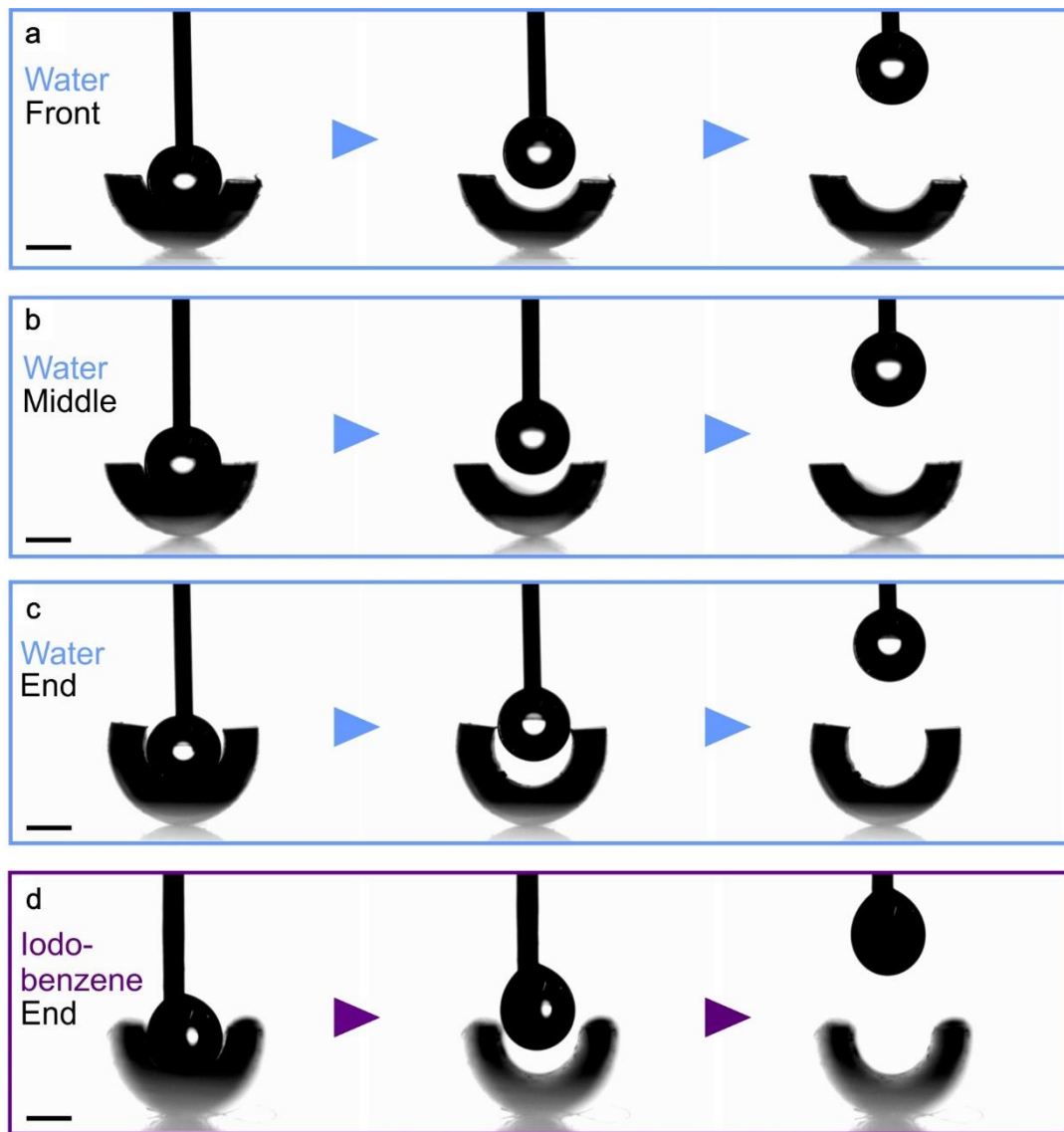


**Figure S16.** Wetting properties at different positions of the coated and fluorinated 2 m LDPE tube. a-c) A 0,5  $\mu$ L water droplet on the coated tube at different positions (front, middle, end); the drops showed very low adhesion and could be easily removed by retracting the syringe. c) A 0.5  $\mu$ L iodobenzene droplet showed low adhesion to the coated tube. Scale bars: 0.5 mm.

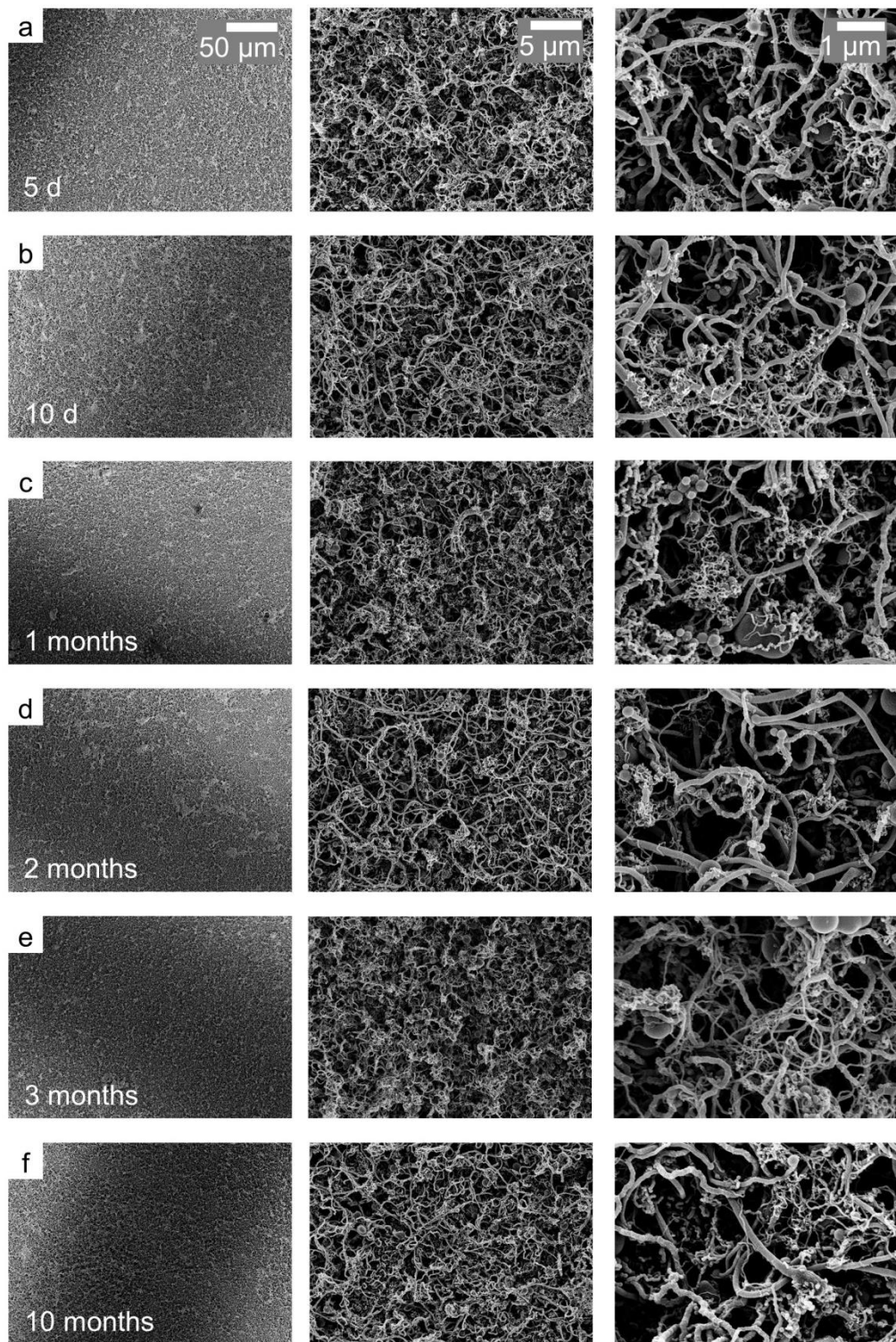


**Figure S16.** SEM images of the inside of coated LDPE tubes after exposure to a water flow with a flow velocity of  $\approx 30 \text{ cm s}^{-1}$ . a) After 5 d exposure. b) After 10 d exposure. c) After 30 d exposure. d) 2 months exposure. e) 3 months exposure. f) 10 months exposure. No visible changes of the coating occurred.

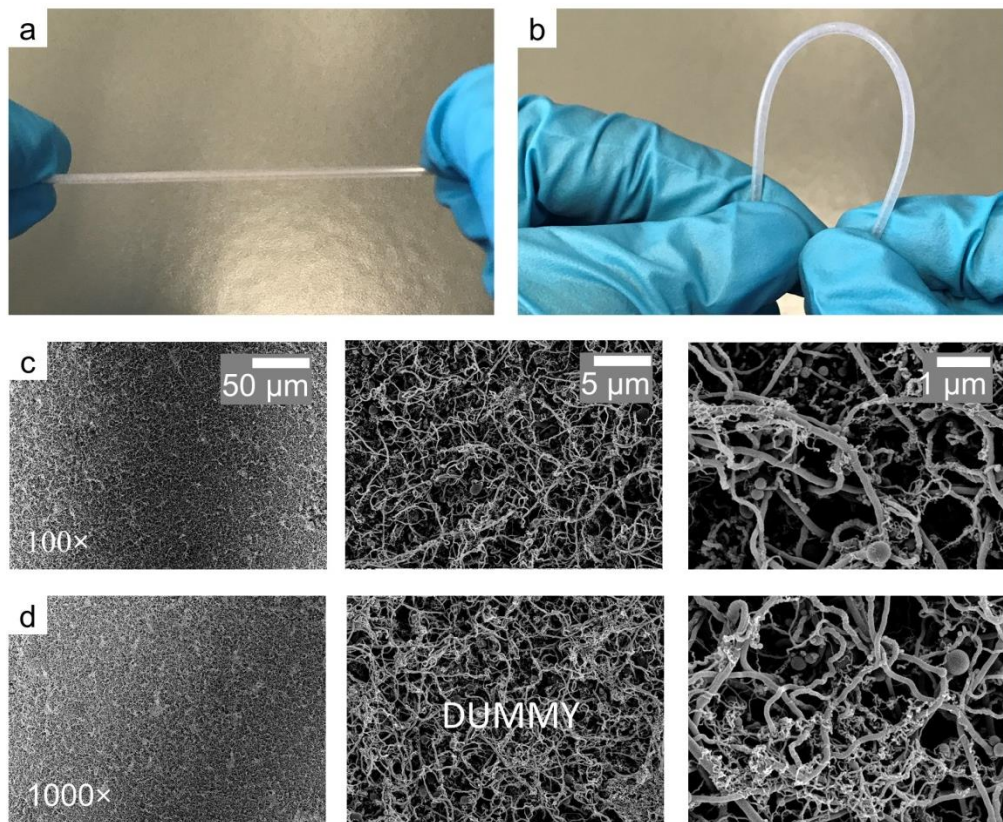


**Figure S17.** Bending experiments. a,b) Photographs of the bending process c,d) SEM images of the inside of coated LDPE tubes after bending for 100 and 1000 times. c) After 100 cycles of bending. d) After 1000 cycles of bending. No damage, delamination or breakage of the coating occurred.

## Experimental Section

### Materials:

If not stated otherwise, experiments were carried out at room temperature. Whole blood was taken at the Department of Transfusion Medicine of the University Medical Center of the JGU Mainz from healthy donors. The study was approved by the local ethics committee and is in accordance with the Declaration of Helsinki. Sodium citrate was added to prevent clotting and plasma was separated by centrifugation. The plasma was pooled and aliquots were stored at -80 °C. A protein concentration of 65-70 g L<sup>-1</sup> was determined by protein assay Pierce 660 nm. Urine was provided by F. Geyer. The following chemicals were used: trichloromethylsilane (99%, Sigma-Aldrich), 1H,1H,2H,2H-perfluorodecyltrichlorosilane (96%, Alfa Aesar), SU-8 305 photoresist (Microchem), mr-Dev 600 developer (micro resist technology), *n*-hexane (99.99%, Fisher Chemical), tetraethoxysilane (TEOS, 98%, Sigma-Aldrich), toluene (99.99%, Fisher Chemical), ethanol (99.8%, Sigma-Aldrich), hexadecane (99%, Sigma-Aldrich), diiodomethane (99%, Sigma-Aldrich), sulfuric acid (99.99%, Sigma-Aldrich), iron sulfate heptahydrate (>99%, Sigma-Aldrich), hydrogen peroxide (35%, VWR), phosphate buffered saline (PBS, Gibco), glutaraldehyde (25 wt%, Sigma-Aldrich). The culture medium, LB (Lysogeny broth) medium, supplemented with Ampicillin (Cat. fas-am-b) was purchased from InvivoGen. Reagents were used as received. Polypropylene (PP, inner diameter (ID): 1.6 mm, outer diameter (OD): 3.2 mm), high-density polyethylene (HDPE, ID: 2.0 mm, OD: 4.0 mm), and low-density poly ethylene (LDPE, ID: 0.95 mm, OD: 2.0 mm) were obtained from RCT Reichelt Chemietechnik. Polyurethane (PU, ID: 1.3 mm, OD: 2.0 mm) and hybrid polyurethane/BaSO<sub>4</sub> (PU/BaSO<sub>4</sub>, ID: 1.4 mm, OD: 2.1 mm) tubes were obtained from B. Braun. Alumina (Al<sub>2</sub>O<sub>3</sub>, ID: 1.5 mm, OD: 2.0 mm; ZrO<sub>2</sub>, ID: 3.0 mm, OD: 6.0 mm) were obtained from Friatec AG. Brass (ID: 2.9 mm, OD: 5.0 mm) and copper (Cu, ID: 2.9 mm, OD: 4.0 mm) tubes were obtained from a local hardware store. Glass slides of 24 × 60 mm<sup>2</sup> and a thickness of 150±5 µm were obtained von Menzel-Gläser.

*Nanofilament-coating of the HDPE, PP, LDPE, and ceramic ( $\text{Al}_2\text{O}_3$  and  $\text{ZrO}_2$ ) tubes using plasma activation:*

The HDPE, PP, LDPE,  $\text{Al}_2\text{O}_3$  and  $\text{ZrO}_2$  tubes were plasma-cleaned and activated in an oxygen plasma chamber using different exposure times ranging from 36 s to 2 min and different powers ranging from 30 W to 120 W (Diener Electronic Femto,  $6 \text{ cm}^3 \text{ min}^{-1}$  oxygen flow rate). Trichloromethylsilane (TCMS) was mixed with toluene having a water content of  $135 \pm 10$  ppm (400  $\mu\text{L}$  TCMS per 100 mL toluene). The water content was evaluated using a Karl Fischer coulometer (Mettler Toledo C20 Compact KF coulometer). The solution was stirred for 60 s. Afterwards, the tubes were immersed in the solution, and the reaction chamber was sealed. After 3 h (20 h for ceramic tubes) the TCMS-coated tubes were rinsed with *n*-hexane and dried under a nitrogen stream.

*Nanofilament-coating of the brass and copper (Cu) tubes:*

The brass and copper (Cu) tubes were cleaned by immersion in a 5 wt% sulfuric acid solution for 30 min. Afterwards the tubes were thoroughly rinsed with deionized water and activated in an oxygen plasma (Diener Electronic Femto, 120 W, 2 min,  $6 \text{ cm}^3 \text{ min}^{-1}$  oxygen flow rate). Trichloromethylsilane (TCMS) was mixed with toluene having a water content of  $225 \pm 5$  ppm (400  $\mu\text{L}$  TCMS per 100 mL toluene). The water content was evaluated using a Karl Fischer coulometer (Mettler Toledo C20 Compact KF coulometer). The solution was stirred for 60 s. Afterwards, the tubes were immersed in the solution, and the reaction chamber was sealed. After 3 h the TCMS-coated tubes were rinsed with *n*-hexane and dried under a nitrogen stream.

*Nanofilament-coating of the PU and PU/BaSO<sub>4</sub> tubes:*

The PU and PU/BaSO<sub>4</sub> tubes were cleaned by flushing with an ethanol/deionized water mixture (50:50 to 40:60). The flushing also leads to adsorption of a thin water layer which is required for nanofilament growth. Trichloromethylsilane (TCMS) was mixed with *n*-hexane having a water content of 85 ppm (200 µL TCMS per 100 mL *n*-hexane). The water content was evaluated using a Karl Fischer coulometer (Mettler Toledo C20 Compact KF coulometer). The solution was stirred for 60 s. After flushing the tubes, they were immediately immersed in the solution, and the reaction chamber was sealed. Alternatively, the solution was injected or pumped through the tube. After 20 h the TCMS-coated tubes were rinsed with *n*-hexane and dried under a nitrogen stream.

*One-step fluorinated nanofilament-coating on HDPE tube:*

The HDPE tube was plasma-cleaned and activated in an oxygen plasma chamber (Diener Electronic Femto, 6 cm<sup>3</sup> min<sup>-1</sup> oxygen flow rate, 150 W, 42 s). Tetraethoxysilane (TEOS, 100 µL, 0.45 mmol) and 1*H*,1*H*,2*H*,2*H*-perfluorodecyltrichlorosilane (PFDTs, 16 µL, 0.048 mmol) was mixed with toluene (80 mL) having a water content of 100±5 ppm. The water content was evaluated using a Karl Fischer coulometer (Mettler Toledo C20 Compact KF coulometer). The solution was stirred for 60 s. Afterwards, the tubes were immersed in the solution and the reaction chamber was sealed. After 20 h the coated tubes were rinsed with *n*-hexane and dried under a nitrogen stream.

*Nanofilament-coated glass slides:*

Glass slides were plasma-cleaned and activated in an oxygen plasma chamber (Diener Electronic Femto, 120 W, 5 min,  $7 \text{ cm}^3 \text{ min}^{-1}$  oxygen flow rate). The activated glass slides were coated with nanofilaments by adding 200  $\mu\text{L}$  of TCMS to a reaction chamber containing 100 mL of *n*-hexane with a water content of  $85\pm5$  ppm. The water content was evaluated using a Karl Fischer coulometer (Mettler Toledo C20 Compact KF coulometer). The solution was stirred for 60 s. Afterwards, the glass slides were immersed in the solution, the reaction chamber was sealed. After 2 d the TCMS-coated glass slides were rinsed with *n*-hexane and dried under a nitrogen stream.

*Nanofilament-coating of tubes using Fenton reaction activation:*

Iron(II) sulfate heptahydrate (0.25 g, 0.90 mmol) was dissolved in 40 mL of deionized water in a reaction vessel having an in- and outlet. The pH of the solution was adjusted to pH = 2.8 using a pH meter by adding sulfuric acid. The mixture was cooled for at least 30 min in an ice bath. The polymeric tube to be activated was connected to the outlet of the reaction vessel using a Tygon connection tube. The end of this polymeric tube was connected to a peristaltic pump (Ismatic Reglo Digital MS-2/12) and finally to the inlet of the reaction vessel using Tygon connection tubes. Hydrogen peroxide (1.8 mL, 35 wt%, 18 mmol) was slowly added to the acidic aqueous ferrous sulfate solution under vigorous stirring, and the mixture was stirred for 10 min. Afterwards, the pump was started using a flow rate of  $8 \text{ mL min}^{-1}$ . The Fenton solution was pumped through the tube for the desired activation time. Typically, the activation time ranged between 20 min and 3 h. Every 15 min the tube was emptied by reversing the pumping direction to eliminate gas bubbles which may form on the inner surface due to the slight oxygen evolution during the Fenton reaction. After the desired activation time was reached, the tube was rinsed by flushing deionized water through the tube. Subsequently, the tube was dried by flushing dry nitrogen and further drying in vacuum. After drying, TCMS was mixed with

toluene having a water content of  $150\pm 5$  ppm (400  $\mu\text{L}$  TCMS per 100 mL toluene) in a reaction vessel having an in- and outlet. The water content was evaluated using a Karl Fischer coulometer (Mettler Toledo C20 Compact KF coulometer). Similar to above, the Fenton-activated tube was connected to the reaction vessel and the pump. Here, Fluran F-5500-A tubes were used to connect the individual parts. After stirring the reaction mixture for 60 s, the reaction vessel was closed, the mixture was pumped into the activated tube, and the pump was stopped for 30 min. Subsequently, the pump was started again for 5 min with a flow rate of 0.1  $\text{mL min}^{-1}$  and stopped again for 45 min. Thereafter, the pumping process was continued for 20 h using a flow rate of 0.1  $\text{mL min}^{-1}$ . Subsequently, the TCMS-coated tubes were rinsed with *n*-hexane and dried under a nitrogen stream.

*Plasma activation of nanofilament-coated surfaces and tubes:*

To activate TCMS-coated surfaces and short tubes, they were exposed to oxygen plasma (Diener Electronic Femto, 120 W, 2 min, 7  $\text{cm}^3 \text{min}^{-1}$  oxygen flow rate).

*Fenton activation of nanofilament-coated surfaces and tubes:*

To activate TCMS-coated surfaces and tubes using Fenton reaction, iron(II) sulfate heptahydrate (2.5 g, 9.0 mmol) was dissolved in 100 mL of deionized water in a reaction vessel. The pH of the solution was adjusted to  $\approx 3$  by adding sulfuric acid. The mixture was cooled in an ice bath. The nanofilament-coated substrate was immersed in EtOH to remove the air cushion of the nanofilaments. Afterwards, it was rinsed with deionized water to remove residual Ethanol. The wet substrate was immersed in the acidic ferrous sulfate solution and hydrogen peroxide (18 mL, 35 wt%, 180 mmol) was slowly added to the solution under vigorous stirring. After 30-60 min the activated substrate was removed from the solution and rinsed with 10 wt% sulfuric acid and copious amounts of deionized water.

*Fluorination of activated nanofilament-coated surfaces and tubes:*

*1H,1H,2H,2H-perfluorodecyltrichlorosilane* was mixed with *n*-hexane (50 µL PFDTs per 100 mL *n*-hexane). The activated tubes and surfaces were immersed in the solution, and the reaction chamber was sealed. Alternatively, the solution was injected or pumped through the tube. After 20 min the fluorinated tubes were rinsed with *n*-hexane and dried under a nitrogen stream.

*Superhydrophobic SU-8 micropillars:*

SU-8 micropillar arrays were prepared on thin glass slides by photolithography. The rectangular pillars were designed 10 µm high with 5×5 µm<sup>2</sup> top areas. The pillar-pillar distance between the centers of two adjacent pillars in a row was 20 µm. The fabrication process consisted of the following steps. First, glass slides were cleaned by ultrasonication in tetrahydrofuran, acetone and ethanol for 15 min, respectively. Then SU-8 photoresist was spin-coated (500 rpm for 5 s followed by 3000 rpm for 30 s, SÜSS MicroTec) on the glass slides. The coated glass slides were heated at 65 °C for 3 min, 95 °C for 10 min and then at 65 °C for 30 min, respectively. Subsequently, the samples were slowly cooled down within two hours and exposed to UV light (mercury lamp, 350 W) under a photolithography mask for 15 s (mask aligner SÜSS MicroTec MJB3 UV400). To cross-link the photoresist, the samples were heated at 65 °C for 3 min, 95 °C for 10 min and 65 °C for 30 min, and then cooled down slowly. Next, the samples were immersed in the SU-8 developer solution for 5 min, washed with isopropanol and then dried in air, resulting in surfaces coated with SU-8 micropillars. The dried samples were plasma-cleaned and activated in an oxygen plasma chamber (Diener Electronic Femto, 30 W, 2 min, 6 cm<sup>3</sup> min<sup>-1</sup> oxygen flow rate). Afterwards, the samples were immersed in a solution containing 50 µL of PFDTs dispersed in 100 mL of *n*-hexane for 20 min. Finally, the fluorinated SU-8 micropillar surfaces were rinsed with *n*-hexane and dried under a nitrogen stream.

*Contact angle measurements and drop observation:*

Receding contact angles were measured using a DataPhysics OCA35 contact angle goniometer. Initially, 6 µL drops were deposited onto the substrate. Afterwards, 20 µL of the liquid was added to and removed from the drop. The measurement was repeated in three different spots per substrate. The error of the receding contact angle measurements was estimated to be  $\pm 4^\circ$ . Roll-off angles were measured using the DataPhysics OCA35 contact angle goniometer. Therefore, 6 µL drops were deposited on the substrates, and the measuring plate was tilted until the drops rolled off. The roll-off angle was determined in at least 6 different spots per substrate and mean roll-off angles and corresponding standard deviations were calculated. The drop adhesion on the coated tubes was observed using the same DataPhysics OCA35 contact angle goniometer. Here, a syringe with a fluorinated tip was used. A 2–3 µL drop was generated at the tip and brought into contact with the coated tube. Afterwards, the syringe was moved up and down to observe the adhesion of the drop to the tube.

*Scanning electron microscopy:*

Scanning electron microscopy (SEM) images were taken with a Zeiss LEO 1530 Gemini SEM at gun voltages of 1.5–3 kV using the in-lens detector. To avoid charging, samples were sputtered with Pt before measurement using a BalTec MED 020 modular high vacuum coating system (with an argon pressure of  $2 \cdot 10^{-5}$  bar and a current of 30 mA, 7 nm Pt).

*X-Ray photoelectron spectroscopy:*

X-ray photoelectron spectra (XPS) were acquired using a Kratos Axis Ultra system. The X-ray source was monochromatic Al-K $\alpha$  (source energy: 1486.69 eV). The take-off angle was 0°. The vacuum in the main chamber was below  $4 \cdot 10^{-10}$  mbar. The hybrid detector mode was used. Survey spectra were recorded with pass energy of 160 eV; high-resolution (narrow range) spectra were recorded with pass energy of 20 eV. Charge neutralization was applied (current: 2.1 A, balance: 2.8 V, bias: 1.3 V). The survey scans were obtained with 2 scans, the high-resolution spectra were obtained with 5 scans. The software CasaXPS (Casa Software Ltd) was used for data elaboration. The binding energies of the XP spectra were calibrated with the help of the aliphatic C1s peak at 285.0 eV. To measure XPS spectra inside of the tubes, the investigated tubes were cut in half horizontally and glued on carbon tape.

*Calculation of the shear rate:*

The flow of a Newtonian liquid through a long cylindrical tube of radius  $r_c$  is given by the Hagen–Poiseuille equation.

$$\frac{dV}{dt} = \frac{\pi \Delta P r_c^4}{8 \eta L}$$

Where  $dV/dt$  is the volume of liquid flowing through the tube per unit of time,  $\Delta P$  pressure drop along the tube of length  $L$  and  $\eta$  is the viscosity of the liquid. The velocity at a distance  $r$  from the center is given by:

$$v(r) = \frac{r_c^2 - r^2}{4 \eta} \frac{\Delta P}{L} = \frac{r_c^2 - r^2}{4\eta} \frac{dV}{dt} \frac{8 \eta}{\pi r_c^4} = \left(1 - \frac{r^2}{r_c^2}\right) \frac{dV}{dt} \frac{2}{\pi r_c^2}$$

The volume flow also follows from the continuity equation:

$$\begin{aligned} \frac{dV}{dt} &= 2\pi \int_0^{r_c} r v(r) dr \\ &= 2\pi v_0 \int_0^{r_c} r \left(1 - \frac{r^2}{r_c^2}\right) dr = 2\pi v_0 \left[\frac{r^2}{2} - \frac{r^4}{4r_c^2}\right]_0^{r_c} = 2\pi v_0 \left(\frac{r_c^2}{2} - \frac{r_c^4}{4r_c^2}\right) = \frac{\pi}{2} v_0 r_c^2 \end{aligned}$$

$$\text{with } v_0 = v(r = 0) = \frac{dV}{dt} \frac{2}{\pi r_c^2}$$

At  $r = r_c$  the shear rate is:

$$\dot{\gamma} = \frac{dv(r = r_c)}{dr} = -\frac{2r_c}{r_c^2} \frac{2}{\pi r_c^2} \frac{dV}{dt} = -\frac{4}{\pi r_c^3} \frac{dV}{dt}$$

For the applied volume flow of  $\frac{dV}{dt} = 11 \text{ mL min}^{-1} = 18 \cdot 10^{-4} \text{ m}^3 \text{ min}^{-1}$  and a tube diameter of  $r_c = 0.475 \text{ mm}$  the shear rate is:

$$|\dot{\gamma}| = \frac{4}{\pi r_c^3} \frac{dV}{dt} = 2.1 \cdot 10^7 \text{ s}^{-1}$$

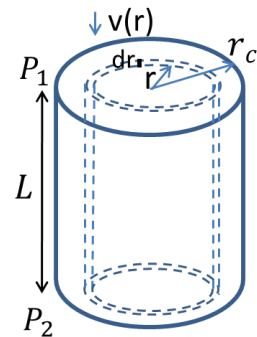


**Figure S18.** Sketch of the tube.

*Bacteria E. coli adhesion testing and imaging:*

The tubes cut in half horizontally were fixed onto a sterile chambered glass with double-sided tape. Each chamber was covered with LB (Lysogeny broth)+Amp medium (1 mL, containing 100 µg mL<sup>-1</sup> of Ampicilin as well as Arabinose added to a final concentration of 0.1%, in the following referred to as LB+Amp medium) containing *E. coli* expressing eGFP (1.0·10<sup>8</sup> cells mL<sup>-1</sup> controlled through OD<sub>600</sub>) and left for incubation at 37 °C for 7 days. The bacterial solution was daily refreshed to avoid nutrient depletion of the bacteria. The bacteria solution for the experiment was prepared by mixing 1 mL of the mother solution containing *E. coli* expressing eGFP with 4 mL of LB+Amp medium, followed by 2 h of incubation at 37 °C at 350 rpm. The optical density of the bacteria-solution was adjusted by dilution with LB+Amp medium. To prepare the samples for SEM investigations, after the 7-day incubation period, the culture medium was carefully removed, and the samples were washed with phosphate buffered saline (PBS, 1 mL, 3 times). The phosphate buffered saline was free of MgCl<sub>2</sub> and CaCl<sub>2</sub>. Adhered bacteria were then fixated by adding a 2.5% (v/v) glutaraldehyde solution in PBS for 30 min at room temperature. The fixative was afterwards removed, and remaining material was washed off by thorough rinsing with buffer solution (PBS, 1 mL, 2 times). Subsequently, the adhered bacteria were dehydrated by successive ethanol soaking (*i.e.*, soaking in water-ethanol mixtures, 25, 50, 60, 70, 80, 90, and 100% (v/v), 15 min each, and last step twice). Then the samples were placed in a vacuum dryer overnight at room temperature. Sterilized consumables were used throughout. To avoid charging, the dried surfaces were sputter-coated with a nm-thick layer of Pt (BalTec MED 020 Modular High Vacuum Coating System, Argon at 2·10<sup>-2</sup> mbar. 7 nm Pt and 30 mA).

*Detection and calculation of average bacteria number on bare and coated PU tubes:*

Based on SEM images, the area covered by bacteria was evaluated using the Analyze Particles plugin of ImageJ. Background subtraction was applied before thresholding to correct for an inhomogeneous background. The threshold was chosen using the default method of imageJ, being a modified IsoData algorithm. Statistics were derived from the evaluation of 14 to 24 images per sample (3 samples in total). The number of bacteria per image (and thus per area) was calculated by dividing the coverage area of the bacteria by the average area of a single bacterium. Afterwards, the average number of bacteria per area of each sample was calculated. Finally, the average number of bacteria per area and corresponding standard deviation based on the samples was calculated. Figure S17 shows an example of this analysis, recognized bacteria areas are highlighted in cyan.

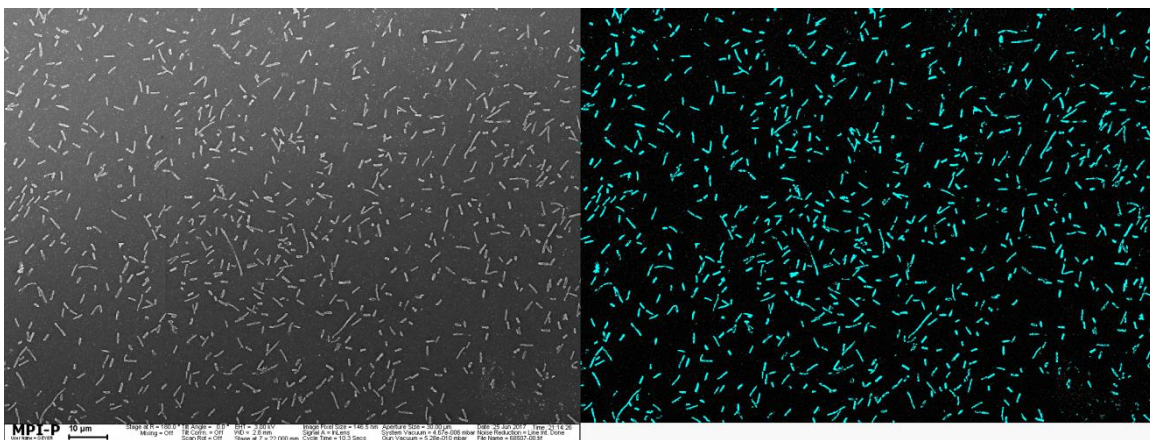


**Figure S19.** SEM image of original data (left) and the recognized bacteria (right, cyan) on a bare PU tube.

Due to the high surface roughness of the nanofilament-coated PU tubes, the bacteria could not reliably be detected using the above-mentioned procedure, therefore bacteria per image (and thus area) were counted manually. Statistics were derived using at least 20 images per samples (2 samples for each nanofilament-coated PU tube). Afterwards, the average number of bacteria per area and the corresponding standard deviation over all samples was calculated.

## Descriptions for the Movies

**Movie S1.** Adhesion experiments of a 2  $\mu\text{L}$  PBS drop on a fluorinated nanofilaments-coated PU/BaSO<sub>4</sub> tube. The drop could be easily removed from the tube by moving the syringe upwards.

**Movie S2.** Adhesion experiments of a 3  $\mu\text{L}$  urine drop on a fluorinated nanofilaments-coated PU/BaSO<sub>4</sub> tube. The drop could be easily removed from the tube by moving the syringe upwards.

**Movie S3.** Adhesion experiments of a 2  $\mu\text{L}$  blood plasma drop on a fluorinated nanofilaments-coated PU/BaSO<sub>4</sub> tube. The drop could be easily removed from the tube by moving the syringe upwards. Some adhesion can be observed at some defects at the cut edge of the tube.

**Movie S4.** Adhesion experiments of a 2  $\mu\text{L}$  diiodomethane drop on a fluorinated nanofilaments-coated PU/BaSO<sub>4</sub> tube. The drop detached from the syringe (due to the high density of diiodomethane; 3.3 g mL<sup>-1</sup>) and rolled out of the tube.

**Movie S5.** Adhesion experiments of a 3  $\mu\text{L}$  water drop on a fluorinated fluorinated SU-8 micropillar arrays ( $9^\circ \pm 1^\circ$  roll-off angle for 6  $\mu\text{L}$  water drops). Upon retraction of the syringe, the drop either stuck to the surface or detachment of the drop from the surface caused visible vibrations of the drop.